Available online at www.sciencedirect.com

ScienceDirect

Geochimica et Cosmochimica Acta 152 (2015) 54–71

Geochimica et Cosmochimica Acta

www.elsevier.com/locate/gca

Stable isotope ratios of nonexchangeable hydrogen in organic matter of soils and plants along a 2100-km climosequence in Argentina: New insights into soil organic matter sources and transformations?

Marc Ruppenthal [a,*], Yvonne Oelmann [a], Héctor Francisco del Valle [b], Wolfgang Wilcke [c]

[a] *Geoecology, Eberhard Karls University Tübingen, Rümelinstrasse 19-23, 72070 Tübingen, Germany*
[b] *Ecología Terrestre, Centro Nacional Patagónico (CENPAT), Consejo Nacional de Investigaciones Científicas y Técnicas (CONICET), Boulevard Brown 2825, U9120ACF Puerto Madryn, Argentina*
[c] *Geographic Institute, University of Berne, Hallerstrasse 12, 3012 Berne, Switzerland*

Received 23 March 2014; accepted in revised form 24 December 2014; available online 7 January 2015

Abstract

The quantitative contribution of shoot and root organic matter (OM) to the soil carbon (C) stock is still unknown, mainly because of methodological restrictions. The novel measurement of the nonexchangeable hydrogen (H) stable isotope ratio (δ^2H_n) in bulk OM provides new opportunities to investigate the sources of soil C and its climate-dependent transformations. Our objectives were to test whether (I) there are systematic differences between δ^2H_n values of aboveground and belowground plant OM and (II) δ^2H_n values of litter and soil OM relate to climate and plant OM source δ^2H_n signals. We determined δ^2H_n values of bulk shoot, root, litter and demineralized soil OM from 20 sampling sites along a 2100-km climosequence from the Argentinean Pampas to the Patagonian steppe. The δ^2H_n values of shoot and litter OM correlated closely with the aridity index ($r = -0.83$, $p < 0.001$ and $r = -0.78$, $p < 0.001$, respectively) because of H isotope fractionation during aridity-controlled transpiration in shoots. In contrast, δ^2H_n values of root and soil OM showed a close correlation with modeled mean annual δ^2H values of local precipitation ($r = 0.91$, $p < 0.001$ and $r = 0.97$, $p < 0.001$, respectively, root mean square error of 8.2‰ and 7.2‰, respectively) and thus mean annual temperature ($r = 0.80$, $p < 0.001$ and $r = 0.88$, $p < 0.001$, respectively). δ^2H_n values of shoot and root OM differed markedly (no linear correlation) most likely because of biosynthetic exchange of C-bound H with ambient water in the roots. δ^2H_n values of root and demineralized soil OM, however, were closely correlated ($r = 0.91$, $p < 0.001$) with a constant offset irrespective of climatic conditions, suggesting that root OM was a more important source of soil OM than shoot OM. A possible contribution of shoot OM to soil OM could only be explained if shoot OM underwent biosynthetic exchange of C-bound H with ambient water in soil during microbial and fungal decomposition. This mechanism is known for substrates processed through the microbial and fungal glycolysis–gluconeogenesis metabolic pathways. Our modeling suggested that the δ^2H_n signature of soil OM is best explained under the assumption that root OM is the predominant source of soil OM, rather than shoot and litter OM.

* Corresponding author. Tel.: +49 7071 29 77527.
E-mail address: marc.ruppenthal@uni-tuebingen.de (M. Ruppenthal).

http://dx.doi.org/10.1016/j.gca.2014.12.024
0016-7037/

1. INTRODUCTION

Soil organic matter (SOM) is the largest pool of terrestrial organic carbon (C) (Jobbagy and Jackson, 2000). Although large proportions of photosynthesized biomass are allocated to roots to guarantee physical anchoring, nutrient acquisition and nutrient and photosynthate storage (Mokany et al., 2006), soil scientists have focused for decades on aboveground inputs of shoot organic matter (OM) as source material for SOM formation (Kleber and Johnson, 2010; Schmidt et al., 2011). Belowground inputs of root OM have not been appropriately considered, which is largely caused by the difficulty of measuring contributions of roots to SOM rather than by a disregard of their importance. A better understanding of the contribution of root OM to SOM formation is therefore crucial for managing soil C stocks and enhancing C sequestration in soils.

Recently, the utilization of C and nitrogen (N) isotopic analyses of bulk shoot, root and soil OM (Bird and Torn, 2006; Katterer et al., 2011) as well as analysis of biomarkers in root and soil OM and their isotopic composition (Mendez-Millan et al., 2010; Mambelli et al., 2011; Hamer et al., 2012) pointed to a more important role of roots for soil OM formation than previously thought (Schmidt et al., 2011). Unfortunately, small contributions of the biomarkers to total OM, low biomarker concentrations and small C and N isotope fractionation in bulk organic matter and individual compounds under control of complex simultaneous processes limit the interpretation of C and N isotope signals. A more promising isotope system is that of H because of the large relative mass difference between the two stable isotopes (^{1}H and ^{2}H) in nature. Utilization of the H isotopic composition of bulk shoot, root and soil OM, however, is still in its infancy and there is a considerable lack of knowledge regarding the controls of the H isotopic composition of bulk soil OM (Schimmelmann et al., 2006). A major problem with the previous use of δ^2H data to trace sources of soil OM has been to obtain accurate δ^2H values without interference of exchangeable H and inorganic H of minerals, i.e., the δ^2H values of nonexchangeable H (δ^2H_n) (Schimmelmann, 1991; Wassenaar and Hobson, 2000; Sauer et al., 2009; Ruppenthal et al., 2013).

It is known that δ^2H values of global precipitation vary systematically (Craig, 1961; Dansgaard, 1964; Bowen, 2012a) and that this variation is reflected in plant OM (Roden et al., 2000; Hayes, 2001). Chemical and biochemical processes usually discriminate against the heavier isotope in the reaction product, thus depleting the reactant in the lighter isotope (Urey and Rittenberg, 1933; Urey, 1947; Bigeleisen, 1965). In photosynthesis, water molecules are split in photosystem II and H from leaf water is transferred to nicotinamide adenine dinucleotide phosphate (NADPH), which enters the Calvin cycle to serve as an electron donor. Here, H from NADPH is transferred to the C_1 position of glyceraldehyde 3-phosphate (GAP), which combines with dihydroxyacetone phosphate (DHAP) to yield fructose and ultimately glucose. Since dissociation of ^1H_2O is favored relative to $^1H^2HO$, transfer of H from water to NADPH strongly discriminates against ^{2}H (Luo et al., 1991), which is in line with the observation that autotrophically produced photosynthate is very depleted in ^{2}H (approx. −170‰) relative to source water (Yakir and DeNiro, 1990). However, this depletion of −170‰ is the net effect of two opposing fractionation mechanisms during photosynthesis: (1) negative H isotope fractionation during incorporation of H into NADPH, which is likely several hundreds of per mil larger than the net fractionation of −170‰ (Luo et al., 1991; Yakir, 1992), and (2) a positive H isotope fractionation of approx. +150‰ associated with exchange reactions of C-bound H in initial photosynthate with cell water, which partially offsets the strongly negative H isotope fractionation at the beginning of the Calvin cycle (Yakir and DeNiro, 1990; Luo and Sternberg, 1992). Although most C-bound H in OM does not spontaneously exchange with environmental water and, in absence of diagenetic alteration, is stable over geologic time scales (Sessions et al., 2004; Schimmelmann et al., 2006), exchange of C-bound H can take place in biosynthetic reactions (Yakir, 1992; Hayes, 2001). In the Calvin cycle, interconversion of DHAP with GAP is associated with enzymatic cleavage of a C–H bond at the C_2 position, and formation of a new C–H bond at the C_1 position. The reaction is catalyzed by triosephosphate isomerase enzymes, which temporarily abstract a C-bound H atom from the substrate (Rose, 1975; Luo and Sternberg, 1992; Yakir, 1992; Berg et al., 2012). This allows for H isotope fractionation effects related to (1) cleavage of the substrate C–H bond, which likely favors cleavage of C–^{1}H relative to C–^{2}H bonds (Yakir, 1992), and (2) isotopic equilibration of the hydrogen nuclei abstracted by the enzyme with hydrogen nuclei in the solvent (Albery and Knowles, 1976; Luo and Sternberg, 1992; Yakir, 1992). Accordingly, it was postulated that the δ^2H value of photosynthates depends on the balance between the two opposing H isotope fractionation effects (Yakir and DeNiro, 1990). For obvious reasons, ^{2}H enrichment of leaf water during transpiration also modifies the precipitation–plant OM relationship of the δ^2H signal (Ziegler et al., 1976; Smith and Ziegler, 1990; Roden et al., 2000; Hayes, 2001).

In post-photosynthetic metabolism, there is further opportunity for exchange of C-bound H of photosynthates. In glycolysis, photosynthesized glucose is not only broken down to gain energy, but also to produce pyruvate, which is the source material for gluconeogenesis and the synthesis of important biomolecules (e.g., polysaccharides, proteins and lipids). In glycolysis as well as gluconeogenesis, interconversion of DHAP with GAP involves cleavage of C–H bonds and therefore partial isotopic equilibration of C-bound H with source water and a positive H isotope fractionation effect in the product relative to the reactant (Yakir and DeNiro, 1990; Luo and Sternberg, 1992; Horita and Vass, 2003; Kreuzer-Martin et al., 2003, 2004). Because glycolysis and gluconeogenesis are the central processes of carbohydrate metabolism shared by all organisms on earth (Berg et al., 2012), exchange of C-bound H with ambient water in heterotrophic biosynthesis can be regarded as universal for all organisms. The possible H isotope fractionations in the formation of organic matter described above are summarized in Fig. 1.

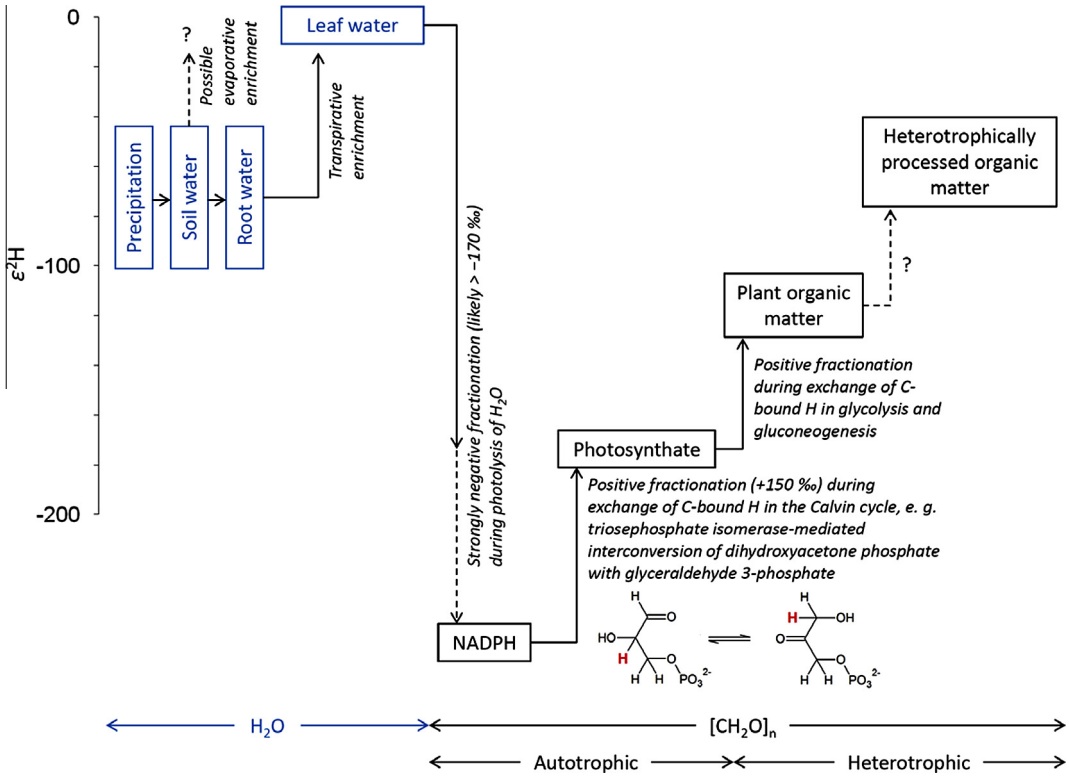

Fig. 1. Schematic representation of possible H isotope fractionations in the formation of organic matter (modified after Yakir (1992) and Hayes (2001)). The major processes of transpirative ^{2}H enrichment in the leaf, ^{2}H depletion during NADPH production and ^{2}H enrichment in post-photosynthetic and heterotrophic metabolism are shown. The uncertainties indicated refer to the possible evaporative enrichment of soil water before root uptake and the uncertain magnitudes of ^{2}H depletion during NADPH production and ^{2}H enrichment during biosynthetic exchange of C-bound H, respectively.

Numerous experiments dedicated to the study of H isotope fractionation in heterotrophic processes have documented incorporation of the H isotopic signature of ambient water into the biosynthesized product, accompanied by positive net H isotope fractionation in the metabolic product (Yakir and DeNiro, 1990; Luo and Sternberg, 1992; Terwilliger and DeNiro, 1995; Horita and Vass, 2003; Kreuzer-Martin et al., 2003, 2004). Luo and Sternberg (1992) reported exchange of about 34% and 67%, respectively, of C-bound H in cellulose with ambient water during heterotrophic growth of grass (*Triticum aestivum* L. and *Hordeum vulgare* L.) seedlings having starch, and castor bean (*Ricinus communis* L.) and peanut (*Arachis hypogaea* L.) seedlings having lipids as the primary substrate. The net H isotope fractionation factors for the addition of C-bound H from water ($\varepsilon^2H_{OM/water}$) during carbohydrate metabolism were +152‰ and +166‰ for the two grass species, and +84‰ and +144‰ for castor bean and peanut, respectively. Yakir and DeNiro (1990) observed approx. 40% exchange of C-bound H with water associated with a $\varepsilon^2H_{OM/water}$ value of +158‰ for cellulose synthesis during heterotrophic growth of the water plant *Lemna gibba* L. Kreuzer-Martin et al. (2003, 2004) showed that during growth of the heterotrophic soil bacterium *Bacillus subtilis* in flasks containing nutrient solutions, 13% and 28% of the C-bound H in logarithmically growing cells and spores, respectively, exchanged with the water used for preparation of the nutrient solution. The respective $\varepsilon^2H_{OM/water}$ values were +122‰ for logarithmically growing cells and +40‰ for spores. Horita and Vass (2003) obtained very similar results (26–28% exchange of C-bound H) growing heterotrophic *Bacillus globigii* and *Erwinia agglomerans* bacteria in nutrient solution. The highest value reported so far for the exchange of C-bound H in heterotrophic biosynthesis came from a study of Terwilliger and DeNiro (1995), who stated that almost all (94%) of the H used for leaf cellulose synthesis exchanged with ambient water (associated with a net H isotope fractionation of +53‰) in avocado seedlings having considerable reserves of stored metabolites. The available studies suggest that heterotrophic biosynthesis is associated with exchange of C-bound H, in most cases in the order of 20–40%, accompanied by a positive $\varepsilon^2H_{OM/water}$ value in the order of +40‰ to +160‰. Although the metabolic pathways of different compound classes are different and cause a large variation in compound-specific δ^2H values (Sternberg et al., 1984; Yakir and DeNiro, 1990), it is remarkable that all above cited studies on biosynthetic H isotope fractionation consistently report isotopic exchange of organically bound H with ambient water. This finding becomes comprehensible when considering the association of glycolysis with the biosynthesis of a wide range of compound classes (e.g., polysaccharides, proteins and lipids), where glycolysis provides metabolites for downstream biosynthetic pathways,

like for example glucose for cellulose synthesis or pyruvate for fatty acid synthesis (Berg et al., 2012). However, our understanding of H isotope fractionation during heterotrophic biosynthesis in different organisms is only at its beginning, especially in the case of microbial and fungal decomposition of OM in soils and sediments.

Currently, it remains unknown how the δ^2H value of plant OM translates into the δ^2H value of soil OM. After incorporation into the soil, δ^2H values of plant OM are potentially modified through microbial and fungal decomposition or leaching of dissolved organic matter, and both processes are known to depend on soil properties and climate (Kalbitz et al., 2000; Raich et al., 2003; Davidson and Janssens, 2006; von Lutzow et al., 2006; Kaiser and Kalbitz, 2012). We are not aware of a previous study addressing H isotope fractionation during decomposition or leaching of terrestrial bulk plant OM. Macko et al. (1983) and Fenton and Ritz (1988) studied the decomposition of seagrass and algae in beakers filled with seawater and found inconsistent results. The results varied from continuously increasing (Macko et al., 1983), to increasing and then decreasing, to unchanged δ^2H values of the decomposing algae (Fenton and Ritz, 1988), depending on the species studied. The results were hypothesized to result from isotopic exchange of (non C-bound) H with surrounding water or preferential loss of ^{1}H during decomposition (Macko et al., 1983), and leaching of isotopically distinct compounds (Fenton and Ritz, 1988), respectively, but both studies ignored the possibility of biosynthetic exchange of C-bound H.

To test the influence of plant OM δ^2H_n signals, soil properties and climate on δ^2H_n values of SOM, a climosequence provides an ideal setting (Schulze et al., 1996; Austin and Sala, 2002; Peri et al., 2012). In the Argentinean Pampas and Patagonia, latitudinal gradients of mean annual temperature, precipitation and δ^2H values of precipitation are among the worldwide most pronounced ones (Hijmans et al., 2005; Bowen, 2012a) and this variation likely affects the H isotopic composition of plant and soil OM.

2. MATERIAL AND METHODS

2.1. Study sites and sampling

Topsoil samples (three replicates each, depth 0–10 to 0–50 cm depending on the thickness of the A horizon), grass shoots, roots and litter were collected at 20 sampling sites along a 2100-km north to south climosequence from the Argentinean Pampas to the Patagonian steppe (Table 1, Fig. 2A, B) in March and April 2010. The climosequence covers a large climate gradient, from warm humid subtropical conditions in the north to warm semiarid and arid conditions in the central part, and warm humid temperate conditions in the south (Peel et al., 2007). Mean annual temperature and precipitation at the sampling sites (Fig. 3B) range from 11.4 to 18.0 °C and 185 mm a^{-1} to 1100 mm a^{-1}, respectively (Instituto Nacional de Technología Agropecuaria, 2012). Modeled estimates of mean annual δ^2H values of precipitation (Bowen, 2012a) showed a systematic trend towards more negative values in the south (Figs. 2A and 3A). The considerable climate-driven variability of characteristic terrestrial ecoregions along the climosequence is depicted in Fig. 2B (Olson et al., 2001). From north to south, the humid Pampas grasslands transition sharply into the semiarid Espinal steppe and shrublands, which form a narrow transition zone to the arid Low Monte semidesert shrublands. Further south, the xerophytic grasslands of the semiarid Patagonian steppe form a large, relatively homogeneous ecoregion (Olson et al., 2001). Soils along the climosequence developed mainly on Quaternary loess in the Pampas (Zarate, 2003) and on Quaternary alluvial sediments in Patagonia (del Valle, 1998; Abraham et al., 2009). Phaeozems, Chernozems and Kastanozems are the dominant soil types in the Pampas and Solonetzes, Calcisols and Luvisols prevail in Patagonia (Instituto Nacional de Technología Agropecuaria, 1990; Dijkshoorn and Huting, 2009). All sampling locations were utilized for more or less intensive livestock farming.

From each of the 20 sampling sites, three replicates of shoot material (only grasses), litter (i.e., the little decomposed plant material on top of the soil constituting the Oi horizon), and A horizons were collected at a distance of ca. 100 m from each other (except for the northernmost Site 1, where only two replicate samples were collected). One replicate sample consisted of homogenized material from several grass plants (at least five) clipped (shoot OM, entire aboveground plant material) or picked from the ground (litter OM) within an area of 5 × 5 m. Dead and live root OM was isolated from the soil samples by hand picking. No litter was found at the two northernmost sites. The sampling sites were between 70 and 160 km apart, depending on the local gradient of modeled mean annual δ^2H values of precipitation (Fig. 2A). Table 1 summarizes selected geographical and climatological properties of the sampling sites and selected chemical properties of shoot, litter, and soil samples.

2.2. Sample processing, demineralization and water steam equilibration

Samples were air-dried during the sampling campaign and later dried at 50 °C in a laboratory drying furnace. Dried soil samples were sieved through a 2 mm sieve. All samples were ground in a ball mill prior to laboratory analysis. Roots picked from the sieved soil samples were washed through gentle shaking in deionized water for one hour inside 50 ml centrifuge tubes. Suspended soil material previously adhering to the root surface was allowed to settle at the bottom of the centrifuge tube over a period of three hours. The roots swimming at the water surface were then decanted and picked with forceps, washed through a 63 μm sieve and dried at 50 °C. A glass electrode (Sentix 81, WTW GmbH, Weilheim, Germany) immersed in a mixture of 10 g of soil and 25 ml of deionized water was used for pH measurement (International Union of Soil Sciences Working Group WRB, 2006). The analysis of δ^2H values of bulk OM is analytically challenging because correction for secondary H exchange is necessary to obtain

Table 1
Selected geographical and climatological properties of the sampling sites and chemical properties of shoot, litter and soil samples. Ecoregion names are abbreviated as follows: HP = humid Pampas, E = Espinal, LM = Low Monte, PS = Patagonian steppe. Values shown represent the mean ± s.d. of three replicates sampled approx. 100 m apart from each other (except for location #1, where only two replicates were collected). The aridity index was calculated as the quotient of mean annual precipitation amount (Instituto Nacional de Tecnología Agropecuaria, 2012) and potential evapotranspiration (P/PET) (Trabucco and Zomer, 2009). The specified predominant graminoids correspond to predominant vegetation at the sampling sites except for Sites 10–15, where *Larrea* and *Geoffroea* sp. (Site 10), *Larrea* sp. (Sites 11–14) and *Stipa* and *Chuquiraga* sp. (Site 15) form the predominant vegetation. We did not have enough sample material to determine the C and N elemental and isotopic composition of root samples.

Location number (north to south)	Geographic latitude	Geographic longitude	Altitude [m a. s. l.]	Ecoregion	Precipitation amount [mm a^{-1}]	Aridity index [P/PET]	Soil type (WRB classification)	Soil pH	Soil C_{org} [g kg^{-1}]	Soil C_{org}/N_{total} ratio	Soil $\delta^{13}C_{org}$ [‰ VPDB]	Soil $\delta^{15}N_{total}$ [‰ air N_2]	Litter C/N ratio	Litter $\delta^{13}C$ [‰ VPDB]	Litter $\delta^{15}N$ [‰ air N_2]	Predominant graminoids	Photo-synthetic mode	Shoot C/N ratio	Shoot $\delta^{13}C$ [‰ VPDB]	Shoot $\delta^{15}N$ [‰ air N_2]
1	32°46′19″S	58°38′11″W	25	HP	1100	0.79	Vertisol	5.3–5.8	17	10.9	−18.3	3.6	N.A.[a]	N.A.	N.A.	*Triticum* sp., *Setaria* sp.	C_3/C_4	22.3	−19.7	3.9
2	34°03′39″S	59°09′30″W	20	HP	1047	0.78	Phaeozem	4.8–5.3	18 ± 2	9.9 ± 0.2	−19.5 ± 0.4	3.6 ± 0.2	N.A.	N.A.	N.A.	*Setaria* sp., *Eragrostis* sp.	C_4	25.1 ± 2.9	−12.0 ± 0.3	4.3 ± 0.6
3	35°18′10″S	58°53′02″W	30	HP	973	0.73	Planosol	5.3–5.9	18 ± 3	9.0 ± 0.2	−22.9 ± 0.3	3.7 ± 1.1	20.5 ± 3.1	−26.3 ± 1.1	2.5 ± 0.3	*Andropogon* sp., *Panicum* sp.	C_4	43.5 ± 5.8	−12.2 ± 0.4	3.6 ± 0.3
4	36°08′50″S	59°16′04″W	40	HP	969	0.74	Phaeozem	5.2–5.7	22 ± 3	10.0 ± 0.4	−22.0 ± 0.4	5.3 ± 1.5	31.4 ± 0.5	−25.5 ± 0.4	1.6 ± 0.9	*Triticum* sp., *Stipa* sp.	C_3	17.6 ± 1.6	−27.7 ± 2.0	3.3 ± 0.8
5	36°52′43″S	59°50′23″W	155	HP	960	0.75	Chernozem	5.1–6.2	39 ± 2	10.5 ± 0.3	−23.2 ± 1.7	6.3 ± 0.7	20.4 ± 1.3	−22.2 ± 2.0	2.6 ± 0.5	*Triticum* sp., *Paspalum* sp.	C_3/C_4	38.7 ± 9.6	−17.3 ± 4.0	2.0 ± 1.7
6	37°20′55″S	60°58′42″W	200	HP	873	0.69	Kastanozem	6.2–7.3	21 ± 2	9.8 ± 0.2	−23.1 ± 0.4	6.5 ± 1.0	25.1 ± 4.4	−22.9 ± 0.8	2.4 ± 0.7	*Festuca* sp., *Panicum* sp.	C_3/C_4	31.6 ± 4.7	−22.6 ± 2.3	3.0 ± 1.1
7	38°08′57″S	61°29′45″W	315	HP	763	0.62	Kastanozem	5.4–6.0	27 ± 6	10.2 ± 0.4	−25.1 ± 0.1	5.9 ± 0.2	14.5 ± 0.7	−27.5 ± 0.8	2.6 ± 0.1	*Festuca* sp.	C_3	13.9 ± 1.8	−28.8 ± 0.6	3.6 ± 0.7
8	38°09′34″S	62°17′15″W	255	HP	728	0.58	Chernozem	6.2–6.7	10 ± 1	9.7 ± 0.6	−22.1 ± 0.7	N.D.[b]	29.4 ± 4.2	−24.1 ± 0.3	−0.3 ± 0.2	*Festuca* sp., *Cenchrus* sp.	C_3/C_4	29.1 ± 1.8	−24.0 ± 0.9	0.8 ± 0.1
9	38°57′51″S	63°51′12″W	100	E	480	0.35	Kastanozem	6.6–7.5	13 ± 1	9.4 ± 0.2	−24.3 ± 0.1	2.6 ± 0.8	32.7 ± 2.2	−26.1 ± 0.3	−2.3 ± 0.4	*Festuca* sp.	C_3	19.0 ± 0.8	−27.8 ± 0.2	2.7 ± 0.9
10	40°10′19″S	64°31′05″W	100	LM	320	0.24	Solonetz	6.9–7.0	9 ± 1	9.2 ± 0.2	−24.8 ± 0.3	2.9 ± 1.0	26.6 ± 1.2	−25.6 ± 0.2	−2.6 ± 0.2	*Stipa* sp.	C_3	15.8 ± 1.4	−25.9 ± 1.1	−0.3 ± 0.4
11	40°48′47″S	65°28′14″W	165	LM	224	0.18	Solonetz	6.7–7.1	6 ± 1	6.1 ± 0.4	−25.3 ± 0.2	2.9 ± 0.5	41.4 ± 7.4	−26.0 ± 0.2	−3.2 ± 1.1	*Stipa* sp.	C_3	15.8 ± 1.4	−27.0 ± 0.5	1.4 ± 1.1
12	41°38′44″S	65°37′51″W	350	LM	193	0.16	Leptosol	7.1–7.3	11 ± 3	7.5 ± 1.4	−24.7 ± 0.2	N.D.	39.7 ± 11.2	−26.1 ± 0.4	−1.3 ± 0.6	*Stipa* sp.	C_3	36.0 ± 7.7	−25.8 ± 0.9	4.0 ± 0.2
13	42°44′45″S	65°39′43″W	120	LM	185	0.16	Calcisol	6.9–7.0	9 ± 2	7.1 ± 0.3	−21.6 ± 0.8	3.0 ± 2.0	51.0 ± 1.8	−24.3 ± 0.4	−1.1 ± 0.8	*Stipa* sp.	C_3	48.0 ± 3.7	−25.7 ± 0.1	0.6 ± 0.2
14	43°40′36″S	65°43′21″W	250	LM	212	0.19	Calcisol	6.6–7.0	6 ± 2	5.8 ± 0.5	−24.1 ± 1.3	4.8 ± 0.7	35.5 ± 7.8	−27.1 ± 0.8	1.1 ± 0.9	*Stipa* sp.	C_3	31.2 ± 1.3	−28.5 ± 0.4	2.8 ± 0.5
15	44°44′29″S	66°39′56″W	455	PS	248	0.25	Solonetz	6.3–6.8	10 ± 1	7.7 ± 0.6	−25.3 ± 0.4	3.0 ± 0.1	48.4 ± 14.8	−26.3 ± 0.7	−0.6 ± 0.5	*Stipa* sp.	C_3	51.4 ± 12.1	−26.7 ± 0.4	0.5 ± 1.1
16	45°31′33″S	67°37′28″W	625	PS	247	0.27	Solonetz	6.8–7.0	11 ± 2	8.8 ± 0.4	−25.8 ± 0.1	2.5 ± 0.2	65.4 ± 4.5	−26.3 ± 0.5	−1.5 ± 0.6	*Stipa* sp.	C_3	67.5 ± 17.4	−26.5 ± 0.5	−1.0 ± 0.8
17	46°23′19″S	68°53′41″W	630	PS	272	0.30	Luvisol	6.5–7.1	14 ± 5	12.9 ± 1.8	−25.4 ± 0.3	N.D.	57.7 ± 17.0	−25.8 ± 0.6	−0.6 ± 1.7	*Stipa* sp.	C_3	62.9 ± 8.6	−26.9 ± 0.9	−0.5 ± 0.6
18	46°55′10″S	69°41′43″W	500	PS	275	0.28	Luvisol	6.8–7.0	8 ± 5	12.8 ± 1.8	−25.2 ± 0.3	N.D.	66.8 ± 17.0	−26.3 ± 0.6	0.0 ± 1.7	*Stipa* sp.	C_3	55.0 ± 8.6	−26.9 ± 0.9	1.2 ± 0.6
19	46°59′15″S	70°41′29″W	735	PS	294	0.36	Vertisol	6.9–7.4	15 ± 2	13.6 ± 0.4	−25.7 ± 0.3	3.5 ± 1.3	57.0 ± 4.8	−26.4 ± 0.3	−0.9 ± 0.9	*Stipa* sp.	C_3	48.0 ± 9.8	−26.1 ± 0.3	0.3 ± 0.6
20	47°24′35″S	70°11′57″W	960	PS	268	0.32	Planosol	6.1–6.7	22 ± 2	12.2 ± 0.3	−24.4 ± 0.4	4.7 ± 0.4	25.5 ± 0.6	−26.5 ± 0.1	2.2 ± 0.5	*Stipa* sp.	C_3	59.0 ± 7.1	−26.7 ± 0.1	1.7 ± 0.5

[a] N.A. is not applicable.
[b] N.D. is not determined.

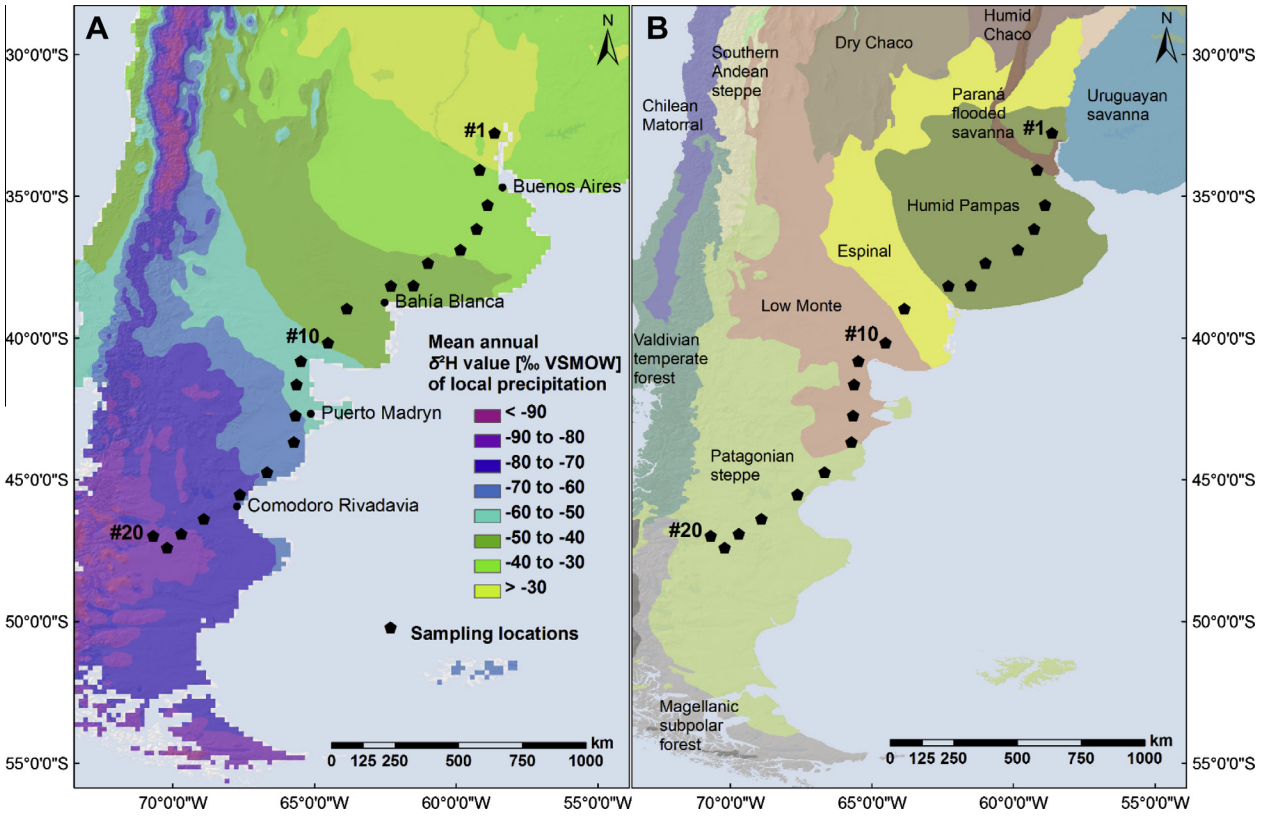

Fig. 2. Map of the sampling locations, modeled mean annual δ^2H value (‰ VSMOW) of precipitation (A) (Bowen, 2012a,b) and terrestrial ecoregions (B) (Olson et al., 2001).

the unbiased isotope ratio of nonexchangeable H (Schimmelmann, 1991; Wassenaar and Hobson, 2000; Sauer et al., 2009). In the case of bulk SOM, analysis of the isotope ratio of nonexchangeable hydrogen (δ^2H_n) is further complicated because SOM and mineral matrix need to be separated. The isolation of SOM for δ^2H_n analysis is necessary to avoid ambiguities in the interpretation of soil δ^2H_n, which constitutes a mixed signal of δ^2H_n of SOM and δ^2H_n of pedogenic clay minerals (Ruppenthal et al., 2010, 2013). Soil samples were thus demineralized according to an optimized procedure which eliminates the influence of inorganic H without affecting the H isotopic composition of SOM (Ruppenthal et al., 2013): 0.5 ± 0.01 g of soil were weighed into 50 ml centrifuge tubes and 40 ± 1 ml of HF (20 vol.%) added. After shaking overnight (approx. 14 h) at room temperature the suspension was centrifuged and the sedimented SOM concentrate was washed three times by resuspension in 0.1 M HCl to remove salts and neoformed fluoride precipitates from the sample, followed once by resuspension in deionized water. To reduce losses of SOM because of solubilization during HF treatment, the HF supernatant was kept for recovery of solubilized SOM using Bond Elut PPL solid phase extraction cartridges (200 mg, Agilent Technologies Inc., USA). The cartridges were preconditioned with acetone and methanol and equilibrated with 0.1 M HCl (one cartridge volume each). After sample addition, the sorbents were washed with 0.1 M HCl and the extracted organic material eluted with methanol followed by acetone (one cartridge volume each). Solubilized SOM recovered from the supernatants in this way was combined with the demineralized particulate SOM concentrate. The combined concentrates were dried at 40 °C and disaggregated in an agate mortar. All chemicals used were of analytical grade. Average C_{org} recovery and C_{org} concentration of demineralized SOM concentrates was $85 \pm 8\%$ and 340 ± 80 g kg^{-1}, respectively. Six (out of 59) SOM concentrates with a C_{org} concentration below 200 g kg^{-1} (indicative of incomplete demineralization) were excluded from further analysis.

The effect of secondary H exchange on δ^2H measurements was corrected by water steam equilibration (Schimmelmann, 1991; Wassenaar and Hobson, 2000; Sauer et al., 2009) of shoot, root, litter, and demineralized soil OM samples with two waters of known H isotopic compositions (-268 ± 1‰ and $+113 \pm 1$‰). The equilibration device used and the detailed procedure are described in Ruppenthal et al. (2013). For calculation of δ^2H_n values we followed the mass balance approach of Schimmelmann (1991), later improved by Schimmelmann et al. (1999) and Wassenaar and Hobson (2000):

$$\delta^2H_n = \frac{\delta^2H_t - 1000x_e(\alpha_{ex\text{-}w} - 1) - x_e\alpha_{ex\text{-}w}\delta^2H_w}{1 - x_e} \quad (1)$$

where $\delta^2H_{t(=total)}$ is the δ^2H value measured for total sample H, x_e is the proportion of total H that has been isotopically exchanged during equilibration, $\alpha_{ex\text{-}w}$ is the equilibrium fractionation factor between the δ^2H value of

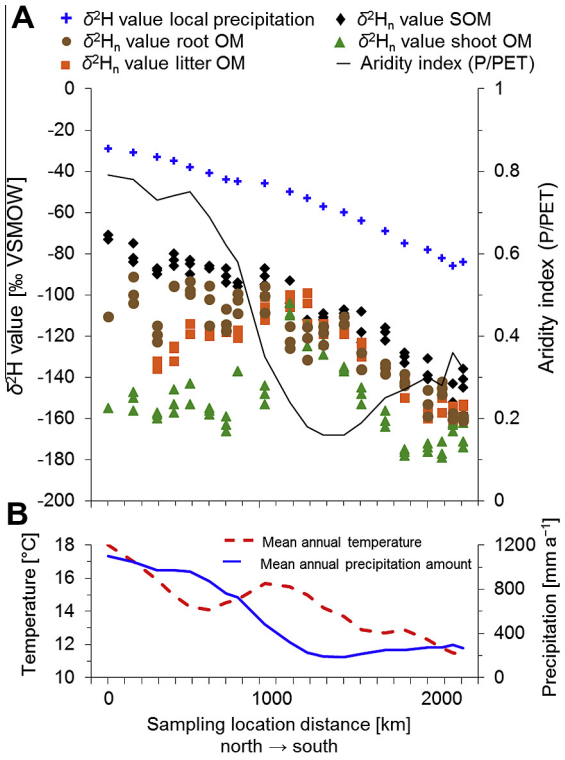

Fig. 3. Modeled mean annual δ^2H values of local precipitation (Bowen, 2012a,b), δ^2H_n values of the different organic matrices sampled (shoot OM ($n = 58$), litter OM ($n = 54$), root OM ($n = 57$) and SOM ($n = 53$)) and the climatic aridity index (A, upper panel) together with mean annual temperature and precipitation amount (B, lower panel) along the climosequence from north (km 0) to south (km 2100).

isotopically exchangeable sample H and equilibration water H, and δ^2H_w is the δ^2H value measured for equilibration water H. A provisional value of 1.08 was assigned to $\alpha_{ex\text{-}w}$ (Schimmelmann, 1991; Schimmelmann et al., 1999; Wassenaar and Hobson, 2000; Sauer et al., 2009). The overall analytical error of δ^2H_n determinations was calculated using Gaussian error propagation as detailed in Ruppenthal et al. (2013). Typical overall analytical errors of replicate samples (including both water steam equilibration and, in case of SOM concentrates, demineralization) were ±3‰ for shoot and soil OM samples and ±4‰ for root and litter OM samples. Error calculation was based on the pooled s.d. of ten independently processed subsamples from four different samples of each organic material, yielding $n = 40$ in total for each organic material.

2.3. EA-IRMS analyses

Concentrations of C were determined with an Elemental Analyzer (EA) (vario EL III, Elementar Analysensysteme, Hanau, Germany). C concentrations measured after combusting the soil samples for 4 h at 550 °C in a muffle furnace (Heiri et al., 2001) were assumed to be inorganic C (C_{inorg}) and organic C (C_{org}) concentrations were calculated as the difference of total C and C_{inorg}. The $\delta^{13}C$ and $\delta^{15}N$ values of shoot, litter and soil OM were determined on a vario EL III EA (Elementar Analysensysteme, Hanau, Germany) coupled to an Isotope Ratio Mass Spectrometer (IRMS) (Isoprime, GV Instruments, Manchester, United Kingdom). Soil samples containing C_{inorg} were decarbonized with sulfurous acid (4 wt.%) according to Verardo et al. (1990) prior to $\delta^{13}C$ measurement to yield the $\delta^{13}C$ value of organic soil C ($\delta^{13}C_{org}$). The procedure allows efficient dissolution of carbonates while largely preserving OM composition (Verardo et al., 1990; Fernandes and Krull, 2008). Total N concentrations (N_{total}) and $\delta^{15}N$ values ($\delta^{15}N_{total}$) were determined without pretreatment for removal of inorganic N because a feasible procedure was not available. Inorganic N might therefore be present at certain locations showing a low soil C_{org}/N_{total} ratio (e.g., in the arid central part of the climosequence, cf. Table 1). Reference materials IAEA-CH-6, IAEA-CH-7, USGS-40 and IAEA-N-2 were used for normalization of measured $\delta^{13}C$ and $\delta^{15}N$ values to the VPDB and AIR-N_2 scales, respectively (Coplen et al., 2006; Paul et al., 2007). Measurement accuracy of IRMS analyses based on routine measurements of interspersed samples of sulfanilic acid (Merck KGaA, Germany) during the 4-month measurement period was ±0.1‰ for $\delta^{13}C$ and ±0.2‰ for $\delta^{15}N$.

2.4. Stable hydrogen isotope ratio analyses

We determined δ^2H values on a vario PyroCube EA (Elementar Analysensysteme, Hanau, Germany) coupled to an IRMS (Isoprime, GV Instruments, Manchester, United Kingdom). The H_3^+ factor varied between 8.19 and 8.34 ppm nA^{-1} over the 4-month measurement period. Two internal laboratory water standards were used for normalization of measured δ^2H values to the VSMOW-SLAP reference scale. The internal laboratory water standards had been calibrated directly against VSMOW2 and SLAP2, using GISP as a measurement accuracy check (Coplen, 1988; Paul et al., 2007), and had δ^2H values of -268 ± 1‰ ($n = 58$) and $+113 \pm 1$‰ ($n = 26$), respectively. Liquid samples were sealed in tin capsules using end cutting pliers and analyzed along with solid samples in the same carousel run, applying the so called "packet dropping" technique (Brand et al., 2009), similar to the approach of Qi et al. (2010). The tin capsules did not have a measurable H_2 blank. The H isotope reference material IAEA-CH-7 with a certified δ^2H value of -100.3 ± 2.0‰ was included in every carousel run as a permanent measurement quality and normalization accuracy control and yielded a δ^2H value of -100 ± 3‰ ($n = 44$).

2.5. Modeled data, statistical evaluations and error calculations

Modeled mean annual δ^2H values of local precipitation at the sampling sites were retrieved from Bowen (2012a,b). The Bowen model is based on data from the IAEA Global Network of Isotopes in Precipitation (GNIP), which unfortunately does not cover Central Patagonia. We therefore reported the uncertainty of modeled mean annual δ^2H values of local precipitation as specified in the Bowen model (2012a,b) in the form of error bars in all figures and

propagated the uncertainties in all calculations involving modeled precipitation δ^2H values. Mean annual precipitation amounts were retrieved from the Argentinean National Institute for Agricultural Technology (Instituto Nacional de Tecnología Agropecuaria, 2012) and values of mean annual potential evapotranspiration from Trabucco and Zomer (2009). Precipitation amount (P) was divided by the value of potential evapotranspiration (PET) to give a climatic aridity index for each sampling location (United Nations Environmental Programme (UNEP), 1992). Modeled mean annual soil respiration CO_2 flux at the sampling sites was retrieved from Raich et al. (2003).

In order to disentangle the effect of changing source water δ^2H values from possible effects of plant physiology and/or climate, we analyzed the differences between δ^2H_n values of the organic materials and the modeled mean annual δ^2H values of precipitation ("net" or "apparent" H isotope fractionation sensu Coplen, (2011)), in addition to the actual δ^2H_n values. If necessary, the systematic change in the H isotopic composition of source water (i.e., precipitation) along the climosequence was factored out in this way. Apparent H isotope fractionation was calculated according to Coplen (2011):

$$\varepsilon^2H_{\text{sample 1/sample 2}} = \alpha^2H_{\text{sample 1/sample 2}} - 1 = \frac{\delta^2H_{\text{sample 1}} + 1}{\delta^2H_{\text{sample 2}} + 1} - 1 \quad (2)$$

where sample 1 and sample 2 specify the compared entities, e.g., the apparent H isotope fractionation between shoot OM and precipitation ($=\varepsilon^2H_{\text{shoot OM/precipitation}}$).

We analyzed the data using independent samples *t*-test, analysis of variance (ANOVA), and Kruskal–Wallis test. We used functional regression (following the geometric mean estimate procedure) instead of ordinary least-squares regression according to the guidelines of Ricker (1973) to account for variability in the independent variable, and to facilitate back-calculation of values of the independent variable from the dependent variable. All data sets were tested for normality using the Shapiro–Wilk test. In regression analyses, scatter plots of standardized predicted values vs. standardized residuals were used to check whether a linear relationship could be assumed. If the assumption of normality was violated for a parametric test, we used a non-parametric counterpart according to the guidelines of Field (2009). If Levene's test showed inhomogeneous variances, Welch's *F* ratio was used to determine the significance of ANOVA (Field, 2009). Because of slight differences in group sizes and unequal variances, we used the Games-Howell post hoc test to identify significant differences among groups. For the Kruskal–Wallis test, Bonferroni-corrected Mann–Whitney tests were used as non-parametric post hoc tests. To indicate the results of statistical comparisons, we used letter coding with the same letters representing non-significant differences and different letters representing significant differences between groups. All statistical analyses were conducted with SPSS 20 (IBM Corp., Armonk, USA) software. All error estimates given are onefold standard deviations (s.d.).

To assess possible changes of the δ^2H_n value of OM during decomposition, we used heterotrophic H exchange as an exemplary process and adapted a mass balance equation published by Yakir and DeNiro (1990) to the case of decomposition of OM:

$$\delta^2H_{n\ \text{product}} = n(\delta^2H_{\text{water}} + \varepsilon^2H_{\text{OM/water}}) + (1-n)\delta^2H_{n\ \text{substrate}} \quad (3)$$

where $\delta^2H_{n\text{substrate}}$ is the initial δ^2H_n value of the decomposing substrate (root or litter OM), $\delta^2H_{n\text{product}}$ is the δ^2H_n value of the decomposition product (SOM), n is the fraction of C-bound H exchanged with water, and $\varepsilon^2H_{\text{OM/water}}$ is the enzyme-mediated net isotopic fractionation between C-bound H in the decomposition product and water during glycolysis–gluconeogenesis metabolism. We made conservative assumptions for the values of n (0.30) and $\varepsilon^2H_{\text{OM/water}}$ (+100‰) based on the available literature (Yakir and DeNiro, 1990; Luo and Sternberg, 1992; Horita and Vass, 2003; Kreuzer-Martin et al., 2003, 2004). However, both values have not yet been determined for the case of OM decomposition under natural conditions.

To account for varying decomposition rates and thus varying magnitudes of heterotrophic incorporation of water H along the climosequence, we extended Eq. (4) to include mean annual soil respiration (Raich et al., 2003) as a proxy for the climate-related decomposition rate:

$$\delta^2H_{n\ \text{product}} = m(n(\delta^2H_{\text{water}} + \varepsilon^2H_{\text{OM/water}}) + (1-n)\delta^2H_{n\ \text{substrate}}) + (1-m) \times \delta^2H_{n\ \text{substrate}} \quad (4)$$

where m is the fraction of total OM undergoing heterotrophic decomposition, varying proportionally to mean annual soil respiration at the sampling site. Since we are not aware of knowledge about the magnitude of net H isotope fractionation effects in relation to turnover rates of OM (here approximated through mean annual soil respiration), we only compared the relative differences in mean annual soil respiration within the climosequence. This was done by assigning the factor 1 to the site with the highest mean annual soil respiration (846 Mg C km^{-2} a^{-1}, Site 1) and proportionally smaller factors to all other sites according to their mean annual soil respiration. The comparably cool and arid Site 17 had the lowest mean annual soil respiration (377 Mg C km^{-2} a^{-1}), thus yielding a proportional factor of 0.44. Because realistically we can only assume partial turnover of litter or root OM entering the soil, the factors entering the model were in fact smaller, e.g., 0.5 and 0.22 for Sites 1 and 17, respectively, when decomposition of 50% of total OM is assumed. A sensitivity test was conducted to assess the uncertainty of precipitation δ^2H values as input variable in the model. The presented model is an attempt to provide proof of concept for the explanation of measured δ^2H_n values of SOM through biosynthetic H isotope exchange with ambient water during SOM decomposition. Current uncertainties in important parameters of the model (i.e., the fraction of C-bound H exchanged with water and the $\varepsilon^2H_{\text{OM/water}}$ value) limit its use for source appointment of SOM at this stage of research.

3. RESULTS

3.1. δ^2H_n values of shoot organic matter

The δ^2H_n values of shoot OM varied between −179‰ and −104‰ and tended to increase from the north to the central part of the climosequence and from there decrease again to the south (Fig. 3). The x_e values of shoot OM were not significantly different from litter OM, but from both root and soil OM (Fig. 4a), and $\varepsilon^2H_{shoot\ OM/precipitation}$ was significantly larger and more variable than in all other types of OM (Fig. 4b). In the humid Pampas where pure C_4 grasslands and mixtures of C_3 and C_4 plants were sampled (Table 1), the values of $\varepsilon^2H_{shoot\ OM/precipitation}$ were significantly correlated with shoot $\delta^{13}C$ values ($y = 1.8x - 64$, $r = 0.89$, $p < 0.001$). The value of $\varepsilon^2H_{shoot\ OM/precipitation}$ was smaller for C_4 than C_3 plants (28‰ on average), with C_4 plants showing significantly less discrimination against ^2H than C_3 plants (−90‰ vs. −118‰, independent t-test, $t(10) = 11.6$, $p < 0.001$). To eliminate the confounding effect of different photosynthetic pathways on δ^2H_n values in the

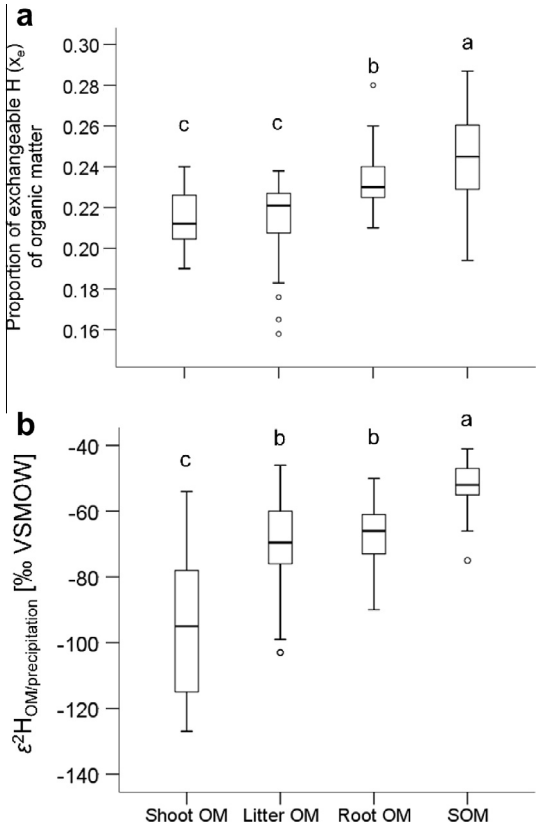

Fig. 4. Box plots of proportions of exchangeable H (a) and $\varepsilon^2H_{OM/precipitation}$ values (b) of the different organic matrices sampled (shoots ($n = 58$), litter ($n = 54$), roots ($n = 57$) and SOM ($n = 53$)). Significant differences between groups were tested with Bonferroni-corrected Mann–Whitney post hoc tests following a Kruskal–Wallis test (a) and Games-Howell post hoc tests following ANOVA (b), respectively. Different letters (a, b, c) indicate significant differences between groups, while the same letters indicate non-significant differences in post hoc comparisons.

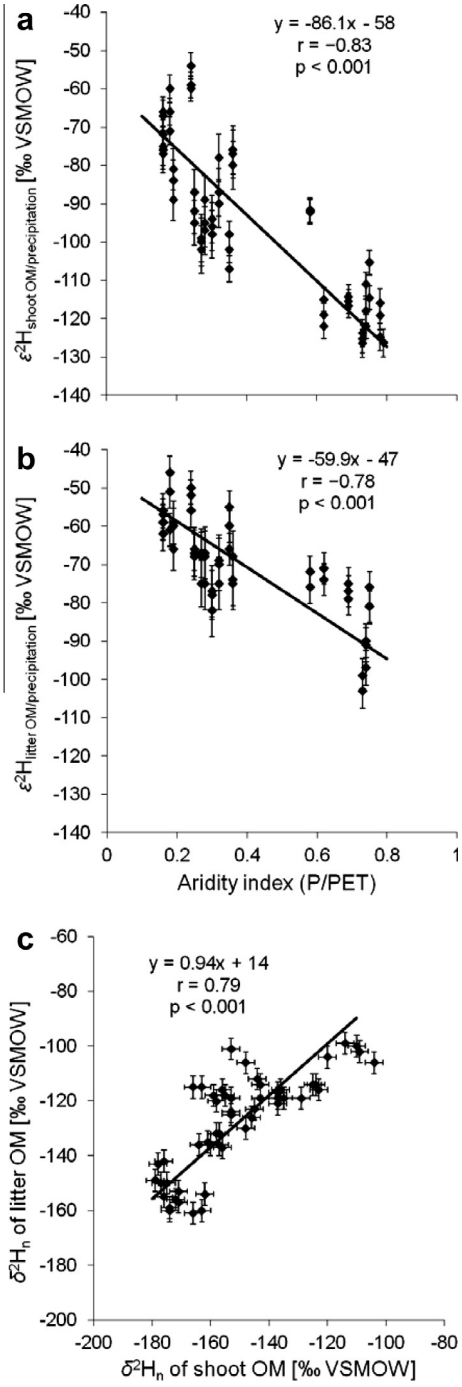

Fig. 5. Regressions of $\varepsilon^2H_{shoot\ OM/precipitation}$ (a) and $\varepsilon^2H_{litter\ OM/precipitation}$ (b) on the aridity index (P/PET). X axis error bars are not shown because of unknown uncertainties for the underlying climate variables (mean annual potential evapotranspiration and precipitation amount) of the aridity index. Y axis error bars show overall s.d. of the apparent H isotope fractionation as evaluated by Gaussian error calculation, including uncertainty associated with modeled precipitation δ^2H values (Bowen, 2012a,b). Unfortunately, aridity indices between approx. 0.4 and 0.6 are not represented by the climosequence because of the abrupt transition between humid Pampas and arid Monte desert, which was not captured by the sampling distance of more than 100 km in this area. Panel (c) shows a regression of δ^2H_n values of litter on shoot OM. Error bars represent the overall uncertainty (±s.d.) of δ^2H_n values of shoot and litter OM, respectively, evaluated by Gaussian error calculation.

ubsequent analysis of a possible aridity effect, we regressed $\varepsilon^2H_{shoot\ OM/precipitation}$ on $\delta^{13}C$ values and corrected samples from those sites with pure C_4 or mixed C_3/C_4 vegetation (Table 1) for their smaller discrimination against ^2H. By subtracting a correction factor according to their $\delta^{13}C$ value (based on the above-mentioned regression), the δ^2H_n values of shoot samples could be recalculated as if all samples originated from C_3 plants. The corrected values of $\varepsilon^2H_{shoot\ OM/precipitation}$ decreased significantly with increasing aridity (Fig. 5a). Similar results were obtained if samples from sites with pure C_4 or mixed C_3/C_4 vegetation were simply discarded from the analysis instead of corrected ($r = 0.77$, $p < 0.001$). There was no linear relationship between δ^2H_n values of shoot OM and δ^2H values of local precipitation (Fig. 6a).

3.2. δ^2H_n values of litter organic matter

δ^2H_n values of litter OM varied between −161‰ and −99‰ and showed a pattern similar to shoot OM along the climosequence (Fig. 3). The x_e values of litter OM were not significantly different from shoot OM, but from both root and soil OM (Fig. 4a). Litter OM was significantly enriched in ^2H relative to shoot OM and variation in $\varepsilon^2H_{litter\ OM/precipitation}$ was significantly reduced relative to $\varepsilon^2H_{shoot\ OM/precipitation}$ (Fig. 4b), but there was a close correlation between δ^2H_n values of litter and shoot OM (Fig. 5c). We found a significant correlation between $\delta^{13}C$ values of shoot and litter OM ($r = 0.87$, $p < 0.001$). Site 3 was the only site where $\delta^{13}C$ values of litter and shoot OM differed markedly (-26.3 ± 1.1‰ vs. -12.2 ± 0.4‰), suggesting a recent transition (from C_3 to C_4) in the grass species sown at this managed pasture. In contrast to shoot OM, the values of $\varepsilon^2H_{litter\ OM/precipitation}$ were not correlated with litter $\delta^{13}C$ values, although some litter samples from the humid Pampas had a $\delta^{13}C$ signature indicating C_4 or mixed C_3/C_4 vegetation (Table 1). Similar to the $\varepsilon^2H_{shoot\ OM/precipitation}$ values those of $\varepsilon^2H_{litter\ OM/precipitation}$ were significantly correlated with the aridity index (Fig. 5b).

3.3. δ^2H_n values of root organic matter

The δ^2H_n values of root OM ranged from −161‰ to −91‰ without much variation in the north of the climosequence and decreasing values in the south (Fig. 3). The x_e values of root OM were significantly higher than those of shoot OM, but significantly lower than those of SOM (Fig. 4a). Root OM was significantly enriched in ^2H relative to shoot OM, the values of $\varepsilon^2H_{root\ OM/precipitation}$ were less variable than those of shoot OM (Figs. 3 and 4b) and there was no linear relationship between δ^2H_n values of root and shoot OM (Fig. 6b). Furthermore, there was neither a significant correlation between $\varepsilon^2H_{root\ OM/precipitation}$ and $\varepsilon^2H_{shoot\ OM/precipitation}$, nor between $\varepsilon^2H_{root\ OM/precipitation}$ and the aridity index. We found a strong correlation between δ^2H_n values of root OM and modeled mean annual δ^2H values of local precipitation (slope of the regression line close to unity, Fig. 7a, root mean square error of 8.2‰) and mean annual temperature (Fig. 7b).

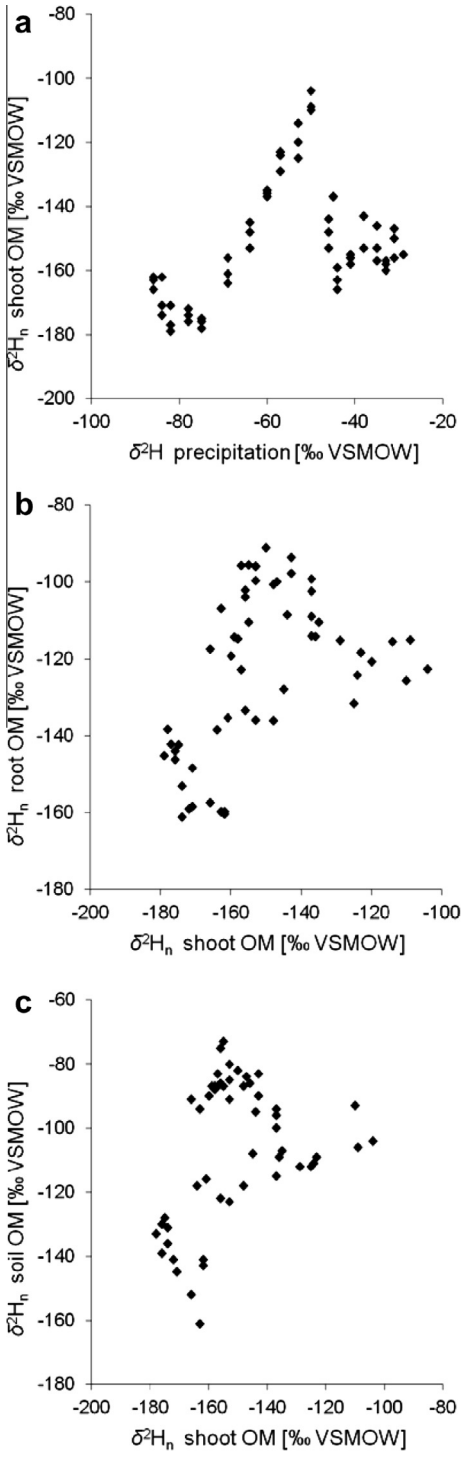

Fig. 6. Relationships between (a) δ^2H_n values of shoot and root OM ($n = 57$), (b) modeled mean annual δ^2H values of local precipitation and δ^2H_n values of shoot OM ($n = 58$), and (c) δ^2H_n values of shoot and soil OM ($n = 52$). Scatter plots of standardized predicted values vs. standardized residuals indicated that the assumption of a linear relationship was not met in any case.

3.4. δ^2H_n values of soil organic matter

In contrast to shoot and litter OM, δ^2H_n values of SOM decreased continuously along the climosequence from

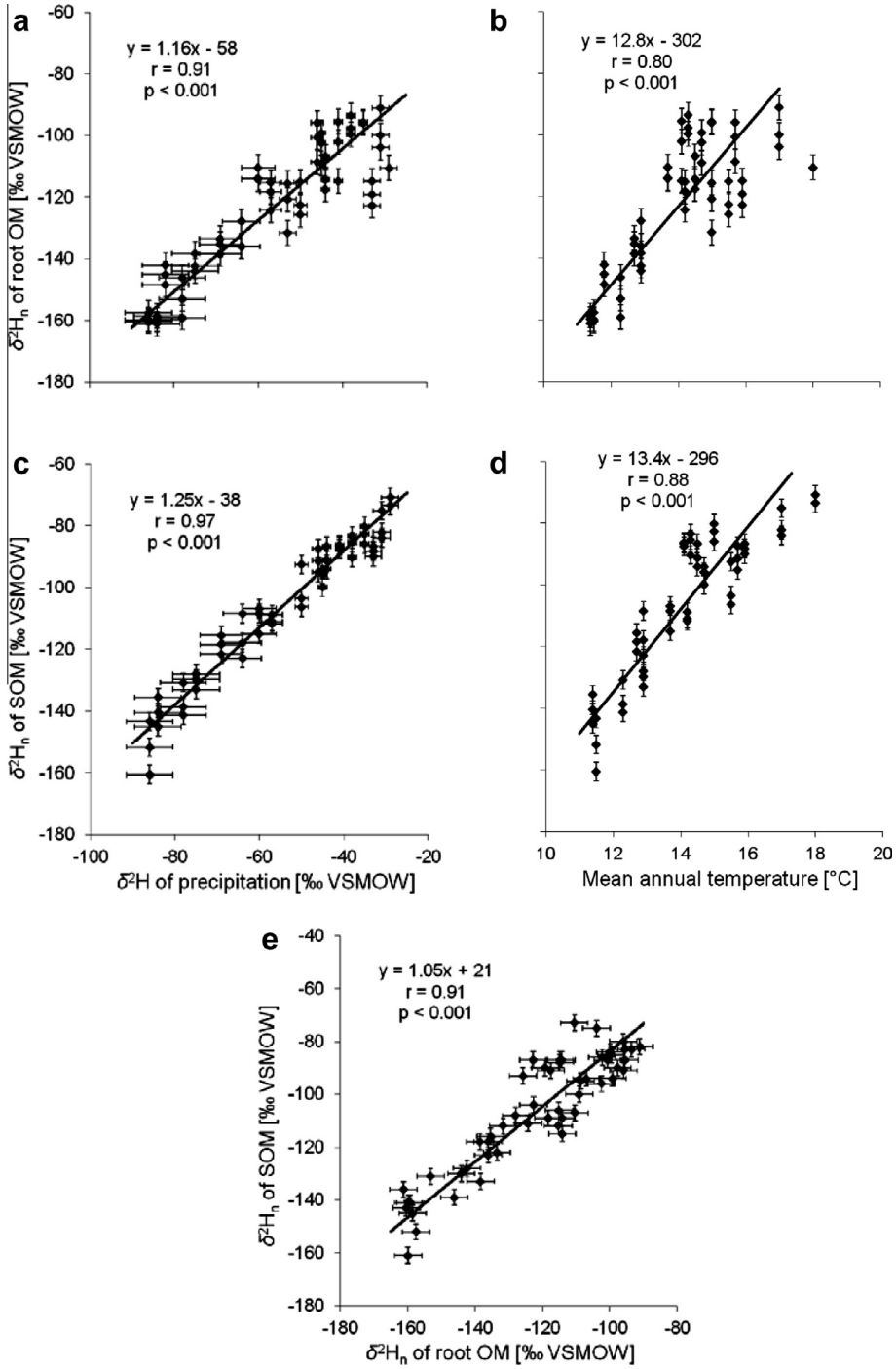

Fig. 7. Regressions of δ^2H_n values of SOM ($n = 53$) on modeled mean annual δ^2H values of local precipitation (a) and mean annual temperature (b), δ^2H_n values of root OM ($n = 54$) on modeled mean annual δ^2H values of local precipitation (c) and mean annual temperature (d), and δ^2H_n values of soil on root OM (e). *X* axis error bars show the uncertainty (±s.d.) of modeled precipitation δ^2H values (Bowen, 2012a,b) (a, c) and δ^2H_n values of root OM (e), respectively. *X* axis error bars are not shown for mean annual temperatures (b, d) due to lack of data. Note the increase of *x* axis error bars along the regression line in (a) and (c), indicating the larger uncertainty of modeled mean annual δ^2H values of local precipitation for sampling locations in Patagonia with large distances to the next Global Network of Isotopes in Precipitation (GNIP) monitoring station. *Y* axis error bars show the overall analytical uncertainty (±s.d.) of δ^2H_n analysis of root and soil OM, respectively, evaluated by Gaussian error calculation.

−161‰ in the north to −71‰ in the south (Fig. 3). The value of $\varepsilon^2H_{SOM/precipitation}$ remained constant throughout the climosequence with a mean value of -51 ± 6‰ (Fig. 4b). The H isotopic composition of SOM resembled that of root OM (Figs. 3 and 4a and b). However, soil and root OM still were significantly different regarding x_e

Table 2
Measured and modeled δ^2H_n values for SOM with litter OM and root OM, respectively, as the decomposing source substrates in the different ecoregions along the climosequence.

Ecoregion	Measured			Modeled	
				Litter OM decomposition	Root OM decomposition
	δ^2H_n litter OM [‰ VSMOW]	δ^2H_n root OM [‰ VSMOW]	δ^2H_n SOM [‰ VSMOW]	δ^2H_n SOM [‰ VSMOW]	δ^2H_n SOM [‰ VSMOW]
Humid Pampas	−122	−105	−89	−97	−85
Espinal and Monte desert	−112	−118	−106	−95	−104
Patagonian steppe	−151	−149	−136	−137	−138

values (because of the more oxidized state of SOM with more hydroxyl and carboxyl functional groups) as well as the apparent H isotope fractionation relative to precipitation (approx. 15‰ offset, Fig. 4a and b). We found a strong correlation between δ^2H_n values of SOM and modeled mean annual δ^2H values of local precipitation (Fig. 7c), suggesting that δ^2H_n values of SOM can be predicted solely from modeled mean annual δ^2H values of local precipitation (94% of variance explained, root mean square error of 7.2‰). Because of the temperature dependence of the H isotopic composition of precipitation, we also found a close correlation between δ^2H_n values of SOM and mean annual temperature (Fig. 7d). There was a close correlation of δ^2H_n values of SOM with root OM with a regression slope close to unity (Fig. 7e), whereas the relationship between SOM and shoot OM clearly deviated from linearity (Fig. 6c). Decomposition of SOM with root OM as the substrate modeled according to Eq. (4) showed a good agreement between measured and modeled δ^2H_n values (Table 2), assuming that a maximum of approx. 50% of initial total root OM underwent decomposition in the humid north and a minimum of approx. 25% in the arid central part of the climosequence to form the current soil OM pool. Modeling results with litter OM as the substrate for SOM formation (assuming decomposition of a maximum of approx. 65% of initial litter OM in the humid north and a minimum of approx. 30% in the arid central part of the climosequence) showed an acceptable agreement between measured and modeled δ^2H_n values (Table 2). However, this model slightly underestimated δ^2H_n values of SOM in the humid Pampas while considerably overestimating them in the Espinal and Monte desert (Table 2).

4. DISCUSSION

4.1. Effects of photosynthetic pathway and aridity on δ^2H_n values of aboveground plant organic matter

Photosynthetic pathway has an influence on the H isotopic composition of plant OM. Previous studies documented a correlation between discrimination against ^2H and discrimination against ^{13}C in bulk OM and cellulose of C_3 and C_4 plants (Ziegler et al., 1976; Sternberg et al., 1984; Leaney et al., 1985). Similarly, we found a close correlation between shoot $\delta^{13}C$ and $\varepsilon^2H_{\text{shoot OM/precipitation}}$ values ($y = 1.8x - 64$, $r = 0.89$, $p < 0.001$). The difference in $\varepsilon^2H_{\text{shoot OM/precipitation}}$ between C_3 and C_4 plants (28‰) observed in our study is close to respective values reported for dicotyledons (41‰ and 30‰) (Ziegler et al., 1976; Leaney et al., 1985) and monocotyledons (15‰) (Leaney et al., 1985). The effect of photosynthetic pathway on δ^2H_n values of shoot OM was hypothesized to be caused by differences in biochemical H isotope fractionation (Ziegler et al., 1976; Smith and Ziegler, 1990) as opposed to differences in transpiration rates of leaf water and thus water-use efficiency (Sternberg et al., 1984). A compelling explanation was provided by Helliker and Ehleringer (2000, 2002), who attributed higher $\delta^{18}O$ values of leaf water and cellulose from C_4 relative to C_3 grasses to the shorter interveinal distance in C_4 grasses, leading to greater back-diffusion of isotopically enriched stomatal water and thus more positive leaf water and cellulose $\delta^{18}O$ values in C_4 grasses. Smith and Freeman (2006) noted that the same mechanism should also affect the H isotopic composition of leaf water, explaining the enrichment of ^2H in *n*-alkanes from C_4 relative to C_3 grasses. We suggest that the H isotopic composition of bulk shoot OM from C_3 and C_4 plants would likewise be affected by the mechanism described by Helliker and Ehleringer (2000, 2002).

Aridity significantly influenced the δ^2H_n values of shoot OM (Figs. 3 and 5a), as expressed by a strong negative correlation between $\varepsilon^2H_{\text{shoot OM/precipitation}}$ and the aridity index (Fig. 5a). The observed enrichment of ^2H at the more arid locations is caused by a larger vapor pressure deficit between leaf stomatal apertures and the surrounding atmosphere, resulting in increased incorporation of ^2H during photosynthesis.(Roden et al., 2000; Hayes, 2001). We are aware of only three prior studies documenting an aridity effect on δ^2H_n values of bulk shoot OM (Ziegler et al., 1976; Rundel et al., 1979; Leaney et al., 1985), but the effect is well documented in compound-specific studies using plant cellulose (Epstein et al., 1977; Yapp and Epstein, 1982) or *n*-alkanes (Smith and Freeman, 2006; Feakins and Sessions, 2010). A close correlation between δ^2H_n values of litter and shoot OM (Fig. 5c) confirmed that the H isotopic composition of shoot OM and its aridity signal were largely preserved in the litter.

The disregard of possible seasonality effects on the H isotopic composition of shoot OM is a limitation of our study. Our study design was not suited for the investigation of seasonality effects, which have recently started to receive increased attention in studies of compound-specific δ^2H_n

values of *n*-alkanes (Sachse et al., 2009; Zech et al., 2011). However, possible seasonality effects might not have a pivotal impact on the interpretation of our results: (I) Many of the sampled grass species are perennial and would therefore likely integrate environmental conditions over more than one year (especially *Festuca* sp. and *Stipa* sp. dominating in the Espinal, Monte desert and Patagonia (cf. Table 1)). In the Pampas on the other hand, the vegetation period is long (270–300 days, van Leeuwen et al. (2013)), indicating that substantial primary production is possible throughout the whole year without a pronounced dormant period. (II) Seasonal variation in primary production is not very pronounced in the grass steppe and shrubland ecosystems along the climosequence (van Leeuwen et al., 2013). In the Espinal, Monte desert and Patagonia, seasonality of the primary production in addition is primarily related to dormant periods of shrub species. Paruelo et al. (1998) noted that grasses show green leaves all year round, without a clear dormant period. (III) The modeled mean annual δ^2H values of precipitation retrieved from Bowen (2012a) represent averages weighted by monthly precipitation amount (Bowen and Revenaugh, 2003). Months with higher precipitation amount therefore have a larger impact in the calculation of the mean annual δ^2H value, which reduces the potential bias from seasonality effects. A seasonality adjustment to the calculated background precipitation δ^2H signature could therefore only be achieved through complete exclusion of certain months from the calculation, but such a procedure could introduce substantial bias, too (e.g., when soil moisture from previous months is tapped at the onset of the vegetation period). For these reasons, we regarded the use of environmental data on an annual timescale as the best compromise between representativeness of the data for as many sampling sites as possible on the one hand, and inevitable regional bias on the other hand. However, appropriate consideration of seasonality effects is important and could be achieved through time-series analyses in future studies.

The difficulty to disentangle climatic effects from effects of plant species composition on δ^2H_n values of shoot OM is another limitation of our study. As species composition depends on climate, no separation of these two effects is possible in a large-scale field study such as ours. Laboratory studies are needed to test net H isotope fractionation effects of different plant species e.g., xerophilic *Stipa* sp. dominating in the Monte desert and Patagonian steppe compared to grass species typical of the humid Pampas.

4.2. Decoupling between δ^2H_n values of aboveground and belowground plant organic matter

In contrast to shoot OM, neither δ^2H_n values of root OM nor $\varepsilon^2H_{\text{root OM/precipitation}}$ were significantly correlated with the aridity index. However, there was a strong and positive correlation between δ^2H values of local precipitation and δ^2H_n values of root OM (Fig. 7a), suggesting that the H isotopic composition of root OM is not considerably influenced by any environmental variables other than the δ^2H value of local precipitation (83% of variance explained, root mean square error of 8.2‰). The δ^2H value of precipitation is mainly controlled by the temperature-dependent equilibrium fractionation between liquid water and water vapor during condensation, and thus correlates with mean annual temperatures (Dansgaard, 1964; Bowen and Revenaugh, 2003). We therefore found a close correlation of δ^2H_n values of root OM with mean annual temperature along the studied climosequence (Fig. 7b). Aridity-driven shoot OM and precipitation-driven root OM δ^2H_n values seem to be decoupled (no linear correlation, Fig. 3 and 6b). This finding is in contrast to expectations, because the biosynthesis of OM in the root is fed from shoot photosynthates, which carry an aridity signal inherited during photosynthesis in the leaf. From studies on the H isotopic composition of plant cellulose it is known that post-photosynthetic processing of photosynthates causes enzyme-mediated, biosynthetic exchange of C-bound H with tissue water in the order of 20–40% (Yakir and DeNiro, 1990; Luo and Sternberg, 1992; Yakir, 1992; Roden et al., 2000; Hayes, 2001). Such an exchange process would attenuate the aridity signal inherited from the incorporation of H from leaf water enriched in ^2H through transpiration. At the same time, biosynthetic exchange of C-bound H would enrich the post-photosynthetic metabolic product in ^2H relative to the initial photosynthates because of a positive net fractionation effect associated with the exchange reaction (Yakir and DeNiro, 1990; Luo and Sternberg, 1992). However, exchange of 20–40% of C-bound H would not result in the complete reset of an aridity signal in post-photosynthetic metabolic reactions, which seems to be the case for root OM (Fig. 7a). We suggest that stored carbohydrates instead of primary photosynthates are used for the biosynthesis of more complex compounds in the roots. If storage carbohydrates are metabolized through the glycolysis–gluconeogenesis pathways, biosynthetic exchange of C-bound H with root tissue water could again enrich the metabolic product in ^2H and push its H isotopic composition still closer to that of the source water (i.e., root tissue water and thus precipitation) (Terwilliger and DeNiro, 1995; Sessions, 2006; DeBond et al., 2013). We therefore suggest that repeated cycles of storage and remobilization of metabolites in the roots resulted in a marked attenuation of the aridity signal inherited during photosynthesis in the shoots and convergence of δ^2H_n values of root OM towards δ^2H values of root tissue water and thus precipitation (Fig. 7a). This mechanism could explain the decoupling of δ^2H_n values of root and shoot OM, the lack of a significant correlation between $\varepsilon^2H_{\text{root OM/precipitation}}$ and the aridity index, and the significant ^2H enrichment of root OM relative to shoot OM (Fig. 4b). Indeed, δ^2H_n values of cellulose, hemicelluloses and lignin in roots have been reported to be enriched in ^2H relative to shoots (Roden et al., 2000; DeBond et al., 2013), which is in line with the ^2H enrichment of bulk root OM observed in our study.

It should be noted that microbial and fungal biomass adhering to root surfaces could create an artifact in the measured root OM δ^2H_n value. Although we cannot rule out the possibility that microbial and fungal biomass still adhered to the root surfaces after washing, it is unlikely that the absolute amount of epibiotic microbial and fungal biomass can be large enough to fully explain the marked decoupling of δ^2H_n values of shoot and root OM.

4.3. Effects of climate and source materials of organic matter on δ^2H_n values of litter and soil organic matter

The δ^2H_n values of SOM were closely correlated with mean annual δ^2H values of local precipitation (taken from Bowen (2012a), Fig. 7c) and thus with mean annual temperature at the sampling site (Fig. 7d). As a consequence, δ^2H_n values of SOM can be predicted solely from modeled mean annual δ^2H values of local precipitation with high precision (94% of variance explained, root mean square error of 7.2‰), while other environmental variables (e.g., aridity, plant species composition, soil type, soil properties, cf. Table 1) have no or only marginal effects on the H isotopic composition of SOM. Hence, the value of $\varepsilon^2H_{SOM/precipitation}$ was remarkably constant along the climosequence (-51 ± 6‰, Fig. 4b) and it was very similar to another recently reported $\varepsilon^2H_{SOM/precipitation}$ value of -46 ± 7‰ for SOM samples from southwest Germany (Ruppenthal et al., 2013). If this holds true globally, the H isotopic composition of precipitation could be inferred from δ^2H_n measurements of SOM and vice versa. Under certain conditions (in situ pedogenesis, no mixing of SOM with different ages), this relationship could eventually be used to constrain the geographical origin of soil samples or to reconstruct paleoenvironmental conditions from thermally immature paleosols.

The strong positive correlation with a slope of the regression line close to unity between δ^2H_n values of SOM and mean annual δ^2H values of local precipitation (Fig. 7a) cannot be explained by the δ^2H_n values of shoot OM as source material for SOM formation. Since the large difference in aridity across the climosequence substantially affected the δ^2H_n values of shoot OM (Figs. 5a and 6a), we would expect an aridity signal in the H isotopic composition of SOM if shoot OM had a substantial contribution to SOM, which was not the case. Interestingly, the δ^2H_n values of root OM not only showed a strong positive correlation with δ^2H values of local precipitation (Fig. 7c), but also with δ^2H_n values of SOM (Fig. 7e). Furthermore, the regression of δ^2H_n values of root OM on δ^2H_n values of SOM had a slope close to unity (Fig. 7e). In contrast, the relationship between δ^2H_n values of shoot OM as a possible source material for SOM formation and δ^2H_n values of SOM clearly deviated from linearity (Fig. 6c). Our results therefore indicate that root OM is a more important source for SOM formation than shoot OM at our study sites. First, grazing activity associated with livestock farming reduces ab initio inputs of litter OM (Carrera et al., 2008; Golluscio et al., 2009) and has been shown to foster root biomass production (Altesor et al., 2006; Derner et al., 2006). Second, a higher likelihood of stabilization through physical protection and organo–mineral interactions of root OM relative to shoot OM leads to selective preservation and thus higher mean residence times of root OM relative to shoot OM (Rasse et al., 2005). This notion is supported by recent biomarker studies identifying root-derived C and root-derived molecular structures as dominant constituents of SOM (Mendez-Millan et al., 2010; Katterer et al., 2011; Mambelli et al., 2011). Based on δ^2H_n values of bulk SOM as quantitative tool to trace sources and sinks of OM, we suggest that plant roots could be more important drivers of soil C sequestration in grass- and shrubland biomes than previously thought.

Although δ^2H_n values of shoot and litter OM as well as root and soil OM were strongly correlated (Figs. 5c and 7e), two systematic differences in δ^2H_n values of litter relative to shoot OM and soil relative to root OM were evident: (1) Litter and soil OM were significantly enriched in ^2H relative to shoot and root OM, respectively, and (2) variation in $\varepsilon^2H_{litter\ OM/precipitation}$ and $\varepsilon^2H_{SOM/precipitation}$, respectively, was significantly lower than in $\varepsilon^2H_{shoot\ OM/precipitation}$ and $\varepsilon^2H_{root\ OM/precipitation}$, respectively (Fig. 4b). These systematic changes of the δ^2H_n value of SOM could be related to turnover effects. We suggest two possible explanations: (1) Selective loss or accumulation of certain organic compounds (carrying a compound-specific δ^2H value) during decomposition could alter the δ^2H_n value or (2) microbial and fungal assimilation and processing could alter the δ^2H_n value via biosynthetic H isotope fractionation.

Many compounds viewed as easily decomposable (e.g., proteins, sugars, cellulose) (Berg and McClaugherty, 2008; Grandy and Neff, 2008) carry higher δ^2H values than bulk OM (Smith and Jacobson, 1976; Hayes, 2001). Preferential loss or leaching of such compounds from litter or soil OM should therefore lead to a depletion of ^2H compared to the source OM (i.e., shoot or litter and root OM, respectively). This is in contrast to our observation (Figs. 3 and 4b). However, to our knowledge, the H isotopic composition of compounds leached from litter or soil OM has never been investigated. We therefore cannot rule out that the observed ^2H enrichment of litter and soil OM compared to source OM is caused by loss or leaching of certain compounds (e.g., lipids) carrying a depleted δ^2H value (Sternberg et al., 1984; Sachse et al., 2012). Similarly, only little is known about the H isotopic composition of compounds eventually accumulating during decomposition relative to source OM, e.g., lignin, cutin and lignin-encrusted carbohydrates (Berg and McClaugherty, 2008; Grandy and Neff, 2008; Preston et al., 2009). We are aware of only three studies reporting δ^2H values for lignin, which is quantitatively the most important compound accumulating relatively during litter decomposition (Berg and McClaugherty, 2008; Wickings et al., 2012). Epstein et al. (1976) and Schmidt et al. (2003) report ^2H enrichment of lignin relative to bulk OM. In contrast, DeBond et al. (2013) in a recent more detailed study report ^2H depletion of lignin relative to bulk OM, which would alter the δ^2H value of litter towards more negative values during decomposition, the opposite of the pattern observed in our study. Because DeBond et al. (2013) present the more compelling data and arguments for a ^2H depletion of lignin, we think that lignin accumulation cannot explain the observed ^2H enrichment of litter and soil OM relative to source OM. In addition, variation in the biomolecular composition of litter and soil OM, respectively, would have to be unrealistically large to account for the strong differences in measured δ^2H_n values along the climosequence. To explain the observed variation of approx. 60‰ in δ^2H_n values of litter and soil OM along the climosequence (Fig. 3), the relative proportions of cellulose and lipids in litter and soil OM,

respectively, would for example have to shift by approx. 30% (assuming a mean δ^2H value difference of approx. 200‰ between cellulose and lipids (Sternberg et al., 1984)). The relative proportions of cellulose and lignin would have to shift by approx. 60% (assuming a mean δ^2H value difference of approx. 100‰ between cellulose and lignin (DeBond et al., 2013)). Such large shifts in the biochemical composition of decomposing litter and soil OM are very unlikely (Preston et al., 2009; Wickings et al., 2012). However, we cannot rule out explanation (1) at the current state of knowledge.

It is known that substrates processed through the heterotrophic glycolysis–gluconeogenesis pathways undergo biosynthetic exchange of C-bound H with ambient water (Yakir and DeNiro, 1990; Luo and Sternberg, 1992; Horita and Vass, 2003; Kreuzer-Martin et al., 2003, 2004). Furthermore, the H isotope fractionation factors associated with biosynthetic exchange of C-bound H in heterotrophic soil bacteria were shown to be strongly positive (+40‰ to +122‰) (Kreuzer-Martin et al., 2003). In our study, precipitation as the dominant source of soil water and tissue water of microorganisms (Kreuzer-Martin et al., 2003, 2004) was considerably enriched in ^2H relative to both shoot and root OM (Figs. 3 and 4b). In addition, the process of incorporation of water H into the biosynthesized product strongly discriminates against ^1H (Kreuzer-Martin et al., 2003). Biosynthetic exchange of C-bound H could therefore lead to ^2H enrichment of decomposing OM. The observed ^2H enrichment of litter and soil OM, respectively, relative to their source OM (i.e., shoot, litter and root OM, respectively, Figs. 3 and 4b) could therefore be explained through explanation (2).

It should be noted that grasses did not form the predominant vegetation in the Low Monte desert (cf. Table 1). It is therefore possible that SOM in this region derives in large part from OM inputs of shrubland species (particularly *Larrea* sp.) which we did not sample. It is likely that aridity would drive the H isotopic composition of aboveground OM of woody plants towards more positive δ^2H_n values, as observed for grasses. However, substantial interspecies differences in net H isotope fractionation effects have been reported for compound-specific δ^2H_n values (Feakins and Sessions, 2010). We therefore cannot rule out that the measured δ^2H_n values of shoot and litter OM are not sufficiently representative for inputs of aboveground OM in the Low Monte desert.

Modeling of decomposition under the assumption of biosynthetic exchange of C-bound H of the source material with ambient water (i.e., precipitation) according to Eq. (4) adequately reproduced the δ^2H_n values of SOM from decomposition of root OM (Table 2). However, decomposition of SOM with litter instead of root OM as the decomposing substrate slightly underestimated δ^2H_n values in the humid Pampas while considerably overestimating them in the Espinal and Monte desert (Table 2). In general, higher decomposition rates (approximated through mean annual soil respiration, cf. Eq. (4)) in the humid Pampas became manifest in a larger magnitude of ^2H enrichment in the model and thus more pronounced shifts towards higher δ^2H_n values of decomposing SOM compared to source OM, relative to the cooler and more arid Patagonian steppe. While uncertainty of modeled precipitation δ^2H values (Bowen, 2012b) had a negligible effect on the modeling results (variation of <1‰), the model was much more sensitive (i.e., variation of up to 20‰) to variations in the fraction of C-bound H exchanged with water and the $\varepsilon^2H_{OM/water}$ value (cf. Eq. (3)). At the present state of knowledge, it is not possible to judge whether these values are eventually subject to substantial interspecies-variability or whether they could be better constrained in future laboratory studies. Because of the possible uncertainties associated with the above-mentioned determining parameters of the model for heterotrophic H exchange, it should be emphasized that the values are not to be regarded as independent proxies for SOM decomposition. We suggest that this application might be possible, but only after the determining parameters (particularly the fraction of C-bound H exchanged with water and the $\varepsilon^2H_{OM/water}$ value) have been constrained better in independent laboratory incubation studies. The sole purpose of the reported model is to highlight that the H isotopic composition of SOM could be explained through heterotrophic H isotope exchange during decomposition. Furthermore, it is important to note that the presented model is simplistic in that it assumes decomposition in steady state condition of only one source material, while in reality decomposition of a mixture of different source materials at variable rates has to be expected. Previous work has shown that turnover of SOM is a multi-layered process complicated by spatial and chemical heterogeneity of the SOM pool and variations in SOM sequestration rates among types of organic matter, soils and ecoregions (Trumbore, 2006; Bol et al., 2009; Trumbore, 2009; Schmidt et al., 2011). None of these important aspects is fully covered by our study, and further research on these topics would likely yield valuable contributions to the understanding of the hydrogen isotope biogeochemistry of plant-soil systems.

5. IMPLICATIONS AND CONCLUSIONS

We found a close relationship between δ^2H values of precipitation and demineralized SOM (root mean square error of 7.2‰) irrespective of climatic and edaphic conditions. We therefore suggest that concerns regarding the robustness of information gained from H isotope analysis of bulk OM in plants and soil (Sachse et al., 2012) can be overcome by use of appropriate analytical methods, including separation of SOM from the mineral matrix and water steam equilibration to remove the influence of exchangeable H. We showed that δ^2H_n values of bulk shoot, root, litter and soil OM differ systematically and can provide valuable information on environmental conditions (isotope hydrology, temperature, aridity), which might be used to reconstruct paleoclimatic conditions from paleosols, to constrain the geographical origin of soil samples, or eventually to trace OM decomposition in the environment. Since δ^2H_n values represent all C-bound H in SOM, our results highlight the importance of root OM for soil OM formation and hence soil C sequestration. Alterations of climatic conditions and resource availability, which influence allocation

of biomass between shoot and root OM (Mokany et al., 2006), are therefore likely to have great effects on soil C sequestration rates. Rising temperatures could for example lead to lower root to shoot ratios in grass- and shrubland biomes and thus cause a positive feedback on climate change (Mokany et al., 2006). The prevalent focus on shoot OM as the major determinant of soil C sequestration should therefore shift towards root OM and its role in soil OM formation.

ACKNOWLEDGMENTS

We thank M. Kersten and N. Groschopf (Johannes Gutenberg University, Mainz) for providing laboratory space and K. Holstein (University of Koblenz), D. Dann and A. Wahl (Eberhard Karls University, Tübingen) for assistance in sample preparation. I. Puentes (Insituto Nacional de Technologia Agropecuaria) greatly helped us by placing regional soil maps at our disposal. We especially thank the late W. Dindorf, B. Müller and M. Müller (Johannes Gutenberg University, Mainz) for advice and assistance in EA-IRMS analyses. We are grateful for funding from the German Science Foundation (DFG, Oe516/2-1).

REFERENCES

Abraham E., del Valle H. F., Roig F., Torres L., Ares J. O., Coronato F. and Godagnone R. (2009) Overview of the geography of the Monte Desert biome (Argentina). *J. Arid Environ.* **73**, 144–153.

Albery W. J. and Knowles J. R. (1976) Deuterium and tritium exchange in enzyme kinetics. *Biochemistry* **15**, 5588–5600.

Altesor A., Pineiro G., Lezama F., Jackson R. B., Sarasola M. and Paruelo J. M. (2006) Ecosystem changes associated with grazing in subhumid South American grasslands. *J. Veg. Sci.* **17**, 323–332.

Austin A. T. and Sala O. E. (2002) Carbon and nitrogen dynamics across a natural precipitation gradient in Patagonia, Argentina. *J. Veg. Sci.* **13**, 351–360.

Berg B. and McClaugherty C. (2008) *Plant Litter. Decomposition, Humus Formation, Carbon Sequestration*, 2nd ed. Springer, Berlin, Heidelberg.

Berg J. M., Tymoczko J. L. and Stryer L. (2012) *Biochemistry*, 7th ed. Freeman, New York.

Bigeleisen J. (1965) Chemistry of isotopes. *Science* **147**, 463–471.

Bird J. A. and Torn M. S. (2006) Fine roots vs. needles: A comparison of C-13 and N-15 dynamics in a ponderosa pine forest soil. *Biogeochemistry* **79**, 361–382.

Bol R., Poirier N., Balesdent J. and Gleixner G. (2009) Molecular turnover time of soil organic matter in particle-size fractions of an arable soil. *Rapid Commun. Mass Spectrom.* **23**, 2551–2558.

Bowen G. J. (2012a) Gridded maps of the isotopic composition of meteoric waters. http://wateriso.eas.purdue.edu/waterisotopes/pages/data_access/ArcGrids.html. (01.08.2012).

Bowen G. J. (2012b) Online isotopes in precipitation calculator (OIPC). http://wateriso.eas.purdue.edu/waterisotopes/pages/data_access/oipc.html. (01.02.2012).

Bowen G. J. and Revenaugh J. (2003) Interpolating the isotopic composition of modern meteoric precipitation. *Water Resour. Res.* **39**, 1–13.

Brand W. A., Coplen T. B., Aerts-Bijma A. T., Bohlke J. K., Gehre M., Geilmann H., Groning M., Jansen H. G., Meijer H. A., Mroczkowski S. J., Qi H., Soergel K., Stuart-Williams H., Weise S. M. and Werner R. A. (2009) Comprehensive inter-laboratory calibration of reference materials for $\delta^{18}O$ versus VSMOW using various on-line high-temperature conversion techniques. *Rapid Commun. Mass Spectrom.* **23**, 999–1019.

Carrera A. L., Bertiller M. B. and Larreguy C. (2008) Leaf litterfall, fine-root production, and decomposition in shrublands with different canopy structure induced by grazing in the Patagonian Monte, Argentina. *Plant Soil* **311**, 39–50.

Coplen T. B. (1988) Normalization of oxygen and hydrogen isotope data. *Chem. Geol.* **72**, 293–297.

Coplen T. B. (2011) Guidelines and recommended terms for expression of stable-isotope-ratio and gas-ratio measurement results. *Rapid Commun. Mass Spectrom.* **25**, 2538–2560.

Coplen T. B., Brand W. A., Gehre M., Groning M., Meijer H. A., Toman B. and Verkouteren R. M. (2006) After two decades a second anchor for the VPDB $\delta^{13}C$ scale. *Rapid Commun. Mass Spectrom.* **20**, 3165–3166.

Craig H. (1961) Isotopic variations in meteoric waters. *Science* **133**, 1702–1703.

Dansgaard W. (1964) Stable isotopes in precipitation. *Tellus* **16**, 436–468.

Davidson E. A. and Janssens I. A. (2006) Temperature sensitivity of soil carbon decomposition and feedbacks to climate change. *Nature* **440**, 165–173.

DeBond N., Fogel M. L., Morrill P. L., Benner R., Bowden R. and Ziegler S. (2013) Variable $\delta^{2}H$ values among major biochemicals in plants: Implications for environmental studies. *Geochim. Cosmochim. Acta* **111**, 117–127.

Del Valle H. F. (1998) Patagonian soils: A regional synthesis. *Ecología Austral* **8**, 103–123.

Derner J. D., Boutton T. W. and Briske D. D. (2006) Grazing and ecosystem carbon storage in the North American Great Plains. *Plant Soil* **280**, 77–90.

Dijkshoorn K. and Huting J. (2009) Soil and terrain database for Argentina. http://www.isric.org/data/soil-and-terrain-data-base-argentina-v1. (01.02.2012).

Epstein S., Yapp C. J. and Hall J. H. (1976) The determination of the D/H ratio of non-exchangeable hydrogen in cellulose extracted from aquatic and land plants. *Earth Planet. Sci. Lett.* **30**, 241–251.

Epstein S., Thompson P. and Yapp C. J. (1977) Oxygen and hydrogen isotope ratios in plant cellulose. *Science* **198**, 1209–1215.

Feakins S. J. and Sessions A. L. (2010) Controls on the D/H ratios of plant leaf waxes in an arid ecosystem. *Geochim. Cosmochim. Acta* **74**, 2128–2141.

Fenton G. E. and Ritz D. A. (1988) Changes in carbon and hydrogen stable isotope ratios of macroalgae and seagrass during decomposition. *Estuar. Coast. Shelf Sci.* **26**, 429–436.

Fernandes M. and Krull E. (2008) How does acid treatment to remove carbonates affect the isotopic and elemental composition of soils and sediments? *Environ. Chem.* **5**, 33–39.

Field A. (2009) *Discovering Statistics Using SPSS*. Sage Publications, London.

Golluscio R. A., Austin A. T., Martinez G. C. G., Gonzalez-Polo M., Sala O. E. and Jackson R. B. (2009) Sheep grazing decreases organic carbon and nitrogen pools in the Patagonian Steppe: Combination of direct and indirect effects. *Ecosystems* **12**, 686–697.

Grandy A. S. and Neff J. C. (2008) Molecular C dynamics downstream: The biochemical decomposition sequence and its impact on soil organic matter structure and function. *Sci. Total Environ.* **404**, 297–307.

Hamer U., Rumpel C. and Dignac M. F. (2012) Cutin and suberin biomarkers as tracers for the turnover of shoot and root derived organic matter along a chronosequence of Ecuadorian pasture soils. *Eur. J. Soil Sci.* **63**, 808–819.

Hayes J. M. (2001) Fractionation of the isotopes of carbon and hydrogen in biosynthetic processes. *Rev. Mineral. Geochem.* **43**, 225–277.

Heiri O., Lotter A. F. and Lemcke G. (2001) Loss on ignition as a method for estimating organic and carbonate content in sediments: Reproducibility and comparability of results. *J. Paleolimnol.* **25**, 101–110.

Helliker B. R. and Ehleringer J. R. (2000) Establishing a grassland signature in veins: ^{18}O in the leaf water of C_3 and C_4 grasses. *Proc. Natl. Acad. Sci. U. S. A.* **97**, 7894–7898.

Helliker B. R. and Ehleringer J. R. (2002) Differential ^{18}O enrichment of leaf cellulose in C_3 versus C_4 grasses. *Funct. Plant Biol.* **29**, 435–442.

Hijmans R. J., Cameron S. E., Parra J. L., Jones P. G. and Jarvis A. (2005) Very high resolution interpolated climate surfaces for global land areas. *Int. J. Climatol.* **25**, 1965–1978.

Horita J. and Vass A. A. (2003) Stable-isotope fingerprints of biological agents as forensic tools. *J. Forensic Sci.* **48**, 122–126.

Instituto Nacional de Technología Agropecuaria (1990) Atlas de suelos de la República Argentina, Buenos Aires.

Instituto Nacional de Technología Agropecuaria (2012) Visualizador integrado GeoINTA. http://geointa.inta.gov.ar/visor/. (01.08.2012).

International Union of Soil Sciences Working Group WRB (2006) World reference base for soil resources 2006. World soil resources report No. 103. ftp://ftp.fao.org/agl/agll/docs/wsrr103e.pdf. (01.02.2012).

Jobbagy E. G. and Jackson R. B. (2000) The vertical distribution of soil organic carbon and its relation to climate and vegetation. *Ecol. Appl.* **10**, 423–436.

Kaiser K. and Kalbitz K. (2012) Cycling downwards – Dissolved organic matter in soils. *Soil Biol. Biochem.* **52**, 29–32.

Kalbitz K., Solinger S., Park J. H., Michalzik B. and Matzner E. (2000) Controls on the dynamics of dissolved organic matter in soils: A review. *Soil Sci.* **165**, 277–304.

Katterer T., Bolinder M. A., Andren O., Kirchmann H. and Menichetti L. (2011) Roots contribute more to refractory soil organic matter than above-ground crop residues, as revealed by a long-term field experiment. *Agric. Ecosyst. Environ.* **141**, 184–192.

Kleber M. and Johnson M. G. (2010) Advances in understanding the molecular structure of soil organic matter. *Adv. Agron.* **106**, 77–142.

Kreuzer-Martin H. W., Chesson L. A., Lott M. J., Dorigan J. V. and Ehleringer J. R. (2004) Stable isotope ratios as a tool in microbial forensics – Part 1. Microbial isotopic composition as a function of growth medium. *J. Forensic Sci.* **49**, 954–960.

Kreuzer-Martin H. W., Lott M. J., Dorigan J. and Ehleringer J. R. (2003) Microbe forensics: Oxygen and hydrogen stable isotope ratios in *Bacillus subtilis* cells and spores. *Proc. Natl. Acad. Sci. U. S. A.* **100**, 815–819.

Leaney F. W., Osmond C. B., Allison G. B. and Ziegler H. (1985) Hydrogen-isotope composition of leaf water in C_3 and C_4 plants: Its relationship to the hydrogen-isotope composition of dry matter. *Planta* **164**, 215–220.

Luo Y. H. and Sternberg L. D. L. (1992) Hydrogen and oxygen isotopic fractionation during heterotrophic cellulose synthesis. *J. Exp. Bot.* **43**, 47–50.

Luo Y. H., Sternberg L., Suda S., Kumazawa S. and Mitsui A. (1991) Extremely low D/H ratios of photoproduced hydrogen by cyanobacteria. *Plant Cell Physiol.* **32**, 897–900.

Macko S. A., Estep M. L. F. and Lee W. Y. (1983) Stable hydrogen isotope analysis of foodwebs on laboratory and field populations of marine amphipods. *J. Exp. Mar. Biol. Ecol.* **72**, 243–249.

Mambelli S., Bird J. A., Gleixner G., Dawson T. E. and Torn M. S. (2011) Relative contribution of foliar and fine root pine litter to the molecular composition of soil organic matter after in situ degradation. *Org. Geochem.*, 1099–1108

Mendez-Millan M., Dignac M. F., Rumpel C., Rasse D. P. and Derenne S. (2010) Molecular dynamics of shoot vs. root biomarkers in an agricultural soil estimated by natural abundance C-13 labelling. *Soil Biol. Biochem.* **42**, 169–177.

Mokany K., Raison R. J. and Prokushkin A. S. (2006) Critical analysis of root:shoot ratios in terrestrial biomes. *Glob. Change Biol.* **12**, 84–96.

Olson D. M., Dinerstein E., Wikramanayake E. D., Burgess N. D., Powell G. V. N., Underwood E. C., D'Amico J. A., Itoua I., Strand H. E., Morrison J. C., Loucks C. J., Allnutt T. F., Ricketts T. H., Kura Y., Lamoreux J. F., Wettengel W. W., Hedao P. and Kassem K. R. (2001) Terrestrial ecoregions of the worlds: A new map of life on Earth. *Bioscience* **51**, 933–938.

Paruelo J. M., Betrán A., Jobbágy E., Sala O. E. and Golluscio R. A. (1998) The climate of Patagonia: General patterns and controls on biotic processes. *Ecología Austral* **8**, 85–101.

Paul D., Skrzypek G. and Forizs I. (2007) Normalization of measured stable isotopic compositions to isotope reference scales – A review. *Rapid Commun. Mass Spectrom.* **21**, 3006–3014.

Peel M. C., Finlayson B. L. and McMahon T. A. (2007) Updated world map of the Koppen–Geiger climate classification. *Hydrol. Earth Syst. Sci.* **11**, 1633–1644.

Peri P. L., Ladd B., Pepper D. A., Bonser S. P., Laffan S. W. and Amelung W. (2012) Carbon ($\delta^{13}C$) and nitrogen ($\delta^{15}N$) stable isotope composition in plant and soil in Southern Patagonia's native forests. *Glob. Change Biol.* **18**, 311–321.

Preston C. M., Nault J. R. and Trofymow J. A. (2009) Chemical changes during 6 years of decomposition of 11 litters in some Canadian forest sites. Part 2. ^{13}C abundance, solid-state ^{13}C NMR spectroscopy and the meaning of "Lignin". *Ecosystems* **12**, 1078–1102.

Qi H., Groning M., Coplen T. B., Buck B., Mroczkowski S. J., Brand W. A., Geilmann H. and Gehre M. (2010) Novel silver-tubing method for quantitative introduction of water into high-temperature conversion systems for stable hydrogen and oxygen isotopic measurements. *Rapid Commun. Mass Spectrom.* **24**, 1821–1827.

Raich J. W., Potter C. S. and Bhagawati D. (2003) Interannual variability in global soil respiration on a 0.5 degree grid cell basis. ORNL/CDIAC-144, NDP-081. http://cdiac.ornl.gov/epubs/ndp/ndp081/ndp081.html. (01.07.2013).

Rasse D. P., Rumpel C. and Dignac M.-F. (2005) Is soil carbon mostly root carbon? Mechanisms for a specific stabilisation. *Plant Soil* **269**, 341–356.

Ricker W. E. (1973) Linear regressions in fishery research. *J. Fish. Res. Board Can.* **30**, 409–434.

Roden J. S., Lin G. G. and Ehleringer J. R. (2000) A mechanistic model for interpretation of hydrogen and oxygen isotope ratios in tree-ring cellulose. *Geochim. Cosmochim. Acta* **64**, 21–35.

Rose I. A. (1975) Mechanism of the aldose–ketose isomerase reactions. *Adv. Enzymol. Relat. Areas Mol. Biol.* **43**, 491–517.

Rundel P. W., Stichler W., Zander R. H. and Ziegler H. (1979) Carbon and hydrogen isotope ratios of bryophytes from arid and humid regions. *Oecologia* **44**, 91–94.

Ruppenthal M., Oelmann Y. and Wilcke W. (2010) Isotope ratios of nonexchangeable hydrogen in soils from different climate zones. *Geoderma* **155**, 231–241.

Ruppenthal M., Oelmann Y. and Wilcke W. (2013) Optimized demineralization technique for the measurement of stable isotope ratios of nonexchangeable H in soil organic matter. *Environ. Sci. Technol.* **47**, 949–957.

Sachse D., Kahmen A. and Gleixner G. (2009) Significant seasonal variation in the hydrogen isotopic composition of leaf-wax lipids for two deciduous tree ecosystems (*Fagus sylvativa* and *Acer pseudoplatanus*). *Org. Geochem.* **40**, 732–742.

Sachse D., Billault I., Bowen G. J., Chikaraishi Y., Dawson T. E., Feakins S. J., Freeman K. H., Magill C. R., McInerney F. A., van der Meer M. T. J., Polissar P., Robins R. J., Sachs J. P., Schmidt H.-L., Sessions A. L., White J. W. C., West J. B. and Kahmen A. (2012) Molecular paleohydrology: Interpreting the hydrogen-isotopic composition of lipid biomarkers from photosynthesizing organisms. *Annu. Rev. Earth Planet. Sci.* **40**, 221–249.

Sauer P. E., Schimmelmann A., Sessions A. L. and Topalov K. (2009) Simplified batch equilibration for D/H determination of non-exchangeable hydrogen in solid organic material. *Rapid Commun. Mass Spectrom.* **23**, 949–956.

Schimmelmann A. (1991) Determination of the concentration and stable isotopic composition of nonexchangeable hydrogen in organic matter. *Anal. Chem.* **63**, 2456–2459.

Schimmelmann A., Lewan M. D. and Wintsch R. P. (1999) D/H isotope ratios of kerogen, bitumen, oil, and water in hydrous pyrolysis of source rocks containing kerogen types I, II, IIS, and III. *Geochim. Cosmochim. Acta* **63**, 3751–3766.

Schimmelmann A., Sessions A. L. and Mastalerz M. (2006) Hydrogen isotopic (D/H) composition of organic matter during diagenesis and thermal maturation. *Annu. Rev. Earth Planet. Sci.* **34**.

Schmidt H.-L., Werner R. A. and Eisenreich W. (2003) Systematics of ^{2}H patterns in natural compounds and its importance for the elucidation of biosynthetic pathways. *Phytochem. Rev.* **2**, 61–85.

Schmidt M. W., Torn M. S., Abiven S., Dittmar T., Guggenberger G., Janssens I. A., Kleber M., Kogel-Knabner I., Lehmann J., Manning D. A., Nannipieri P., Rasse D. P., Weiner S. and Trumbore S. E. (2011) Persistence of soil organic matter as an ecosystem property. *Nature* **478**, 49–56.

Schulze E. D., Mooney H. A., Sala O. E., Jobbagy E., Buchmann N., Bauer G., Canadell J., Jackson R. B., Loreti J., Oesterheld M. and Ehleringer J. R. (1996) Rooting depth, water availability, and vegetation cover along an aridity gradient in Patagonia. *Oecologia* **108**, 503–511.

Sessions A. L. (2006) Seasonal changes in D/H fractionation accompanying lipid biosynthesis in *Spartina alterniflora*. *Geochim. Cosmochim. Acta* **70**, 2153–2162.

Sessions A. L., Sylva S. P., Summons R. E. and Hayes J. M. (2004) Isotopic exchange of carbon-bound hydrogen over geologic timescales. *Geochim. Cosmochim. Acta* **68**, 1545–1559.

Smith F. A. and Freeman K. H. (2006) Influence of physiology and climate on δD of leaf wax n-alkanes from C_3 and C_4 grasses. *Geochim. Cosmochim. Acta* **70**, 1172–1187.

Smith B. N. and Jacobson B. S. (1976) $^{2}H/^{1}H$ and $^{13}C/^{12}C$ ratios for classes of compounds isolated from potato tuber. *Plant Cell Physiol.* **17**, 1089–1092.

Smith B. N. and Ziegler H. (1990) Isotopic fractionation of hydrogen in plants. *Bot. Acta* **103**, 335–342.

Sternberg L. O., DeNiro M. J. and Johnson H. B. (1984) Isotope ratios of cellulose from plants having different photosynthetic pathways. *Plant Physiol.* **74**, 557–561.

Terwilliger V. J. and DeNiro M. J. (1995) Hydrogen isotope fractionation in wood-producing avocado seedlings: Biological constraints to paleoclimatic interpretations of δD values in tree ring cellulose. *Geochim. Cosmochim. Acta* **59**, 5199–5207.

Trabucco A. and Zomer R. J. (2009) Global aridity index (Global-Aridity) and global potential evapo-transpiration (Global-PET) geospatial database. CGIAR Consortium for Spatial Information. http://csi.cgiar.org/Aridity/. (01.08.2012).

Trumbore S. (2006) Carbon respired by terrestrial ecosystems – Recent progress and challenges. *Glob. Change Biol.* **12**, 141–153.

Trumbore S. (2009) Radiocarbon and soil carbon dynamics. *Annu. Rev. Earth Planet. Sci.* **37**, 47–66.

United Nations Environmental Programme (UNEP) (1992) *World Atlas of Desertification*. Arnold, E., London.

Urey H. C. (1947) The thermodynamic properties of isotopic substances. *J. Chem. Soc.*, 562–581

Urey H. C. and Rittenberg D. (1933) Some thermodynamic properties of the $H^{1}H^{2}$, $H^{2}H^{2}$ molecules and compounds containing the H^{2} atom. *J. Chem. Phys.* **1**, 137–143.

van Leeuwen W. J. D., Hartfield K., Miranda M. and Meza F. J. (2013) Trends and ENSO/AAO driven variability in NDVI derived productivity and phenology alongside the Andes Mountains. *Remote Sens.* **5**, 1177–1203.

Verardo D. J., Froehlich P. N. and McIntyre A. (1990) Determination of organic carbon and nitrogen in marine sediments using the Carlo Erba NA-1500 Analyzer. *Deep-Sea Res.* **37**, 157–165.

von Lutzow M., Kogel-Knabner I., Ekschmitt K., Matzner E., Guggenberger G., Marschner B. and Flessa H. (2006) Stabilization of organic matter in temperate soils: Mechanisms and their relevance under different soil conditions – A review. *Eur. J. Soil Sci.* **57**, 426–445.

Wassenaar L. I. and Hobson K. A. (2000) Improved method for determining the stable-hydrogen isotopic composition (δD) of complex organic materials of environmental interest. *Environ. Sci. Technol.* **34**, 2354–2360.

Wickings K., Grandy A. S., Reed S. C. and Cleveland C. C. (2012) The origin of litter chemical complexity during decomposition. *Ecol. Lett.* **15**, 1180–1188.

Yakir D. (1992) Variations in the natural abundance of oxygen-18 and deuterium in plant carbohydrates. *Plant Cell Environ.* **15**, 1005–1020.

Yakir D. and DeNiro M. J. (1990) Oxygen and hydrogen isotope fractionation during cellulose metabolism in *Lemna gibba* L. *Plant Physiol.* **93**, 325–332.

Yapp C. J. and Epstein S. (1982) A reexamination of cellulose carbon-bound hydrogen δD measurements and some factors affecting plant-water D/H relationships. *Geochim. Cosmochim. Acta* **46**, 955–965.

Zarate M. A. (2003) Loess of southern South America. *Quatern. Sci. Rev.* **22**, 1987–2006.

Zech M., Pedentchouk N., Buggle B., Leiber K., Kalbitz K., Marković S. B. and Glaser B. (2011) Effect of leaf litter degradation and seasonality on D/H isotope ratios of n-alkane biomarkers. *Geochim. Cosmochim. Acta* **75**, 4917–4928.

Ziegler H., Osmond C. B., Stichler W. and Trimborn P. (1976) Hydrogen isotope discrimination in higher plants: Correlations with photosynthetic pathway and environment. *Planta* **128**, 85–92.

Associate editor: Thomas S. Bianchi